Timelines of plume characteristics of the Hunga Tonga-Hunga Ha'apai eruption sequence from 19 December 2021 to 16 January 2022: Himawari-8 observations

Authors: Ashok Kumar Gupta[1*], Ralf Bennartz[1,2], Kristen E. Fauria[1], Tushar Mittal[3,4]

Affiliations:

[1]Department of Earth and Environmental Sciences, Vanderbilt University; Nashville, Tennessee, USA

[2]Space Science and Engineering Center, University of Wisconsin - Madison, Wisconsin, USA

[3]Department of Earth, Atmospheric and Planetary Sciences, Massachusetts Institute of Technology, Cambridge, Massachusetts, USA

[4]Department of Geosciences, Pennsylvania State University, Pennsylvania, USA

***Corresponding author. Email:** ashok.k.gupta@vanderbilt.edu

Abstract:

The 15 January 2022 Hunga Tonga-Hunga Ha'apai (HTHH) eruption was preceded by large eruptions on 19 December 2021 and 13 January 2022. We present the evolution of umbrella cloud top height for all three major HTHH eruptions using satellite remote sensing. We also determined the umbrella clouds' radial expansion and volumetric flow rates (VFR) and confirmed that the umbrellas on all three dates contained significant water and ice. Additionally, we identified two umbrella clouds at distinct elevations on 15 January 2022. Specifically, after 05:30 UTC, the strong westward propagation of an upper umbrella (U_B) cloud at 31 km $\pm$ 1–3km enabled the visibility of the lower umbrella (U_A) cloud at 17 km $\pm$ 1–2km. The satellite-derived VFR for 15 January 2022 was 5.0 $\pm$ 1.0 x 10^{11} m^3s^{-1}, nearly two orders of magnitude higher than the VFRs estimated for the 19 December 2021 and 13 January 2022 eruptions.

Main Text

On 15 January 2022, between 04:00-04:10 UTC, the shallow water Hunga Tonga-Hunga Ha'apai (referred as, "HTHH") (175.38°W, 20.57°S) volcano, constituted one of the century's most explosive submarine eruptions. The ashfall and tsunamis produced by the eruption severely affected the Kingdom of Tonga and surrounding regions[1,2,3,4,5,6]. Lamb waves produced by the HTHH eruption circled multiple times around the globe[5] and the highest plume reached approximately 55-58 km[7,8]. The height of the plume and umbrella region, the area where the volcanic cloud spreads laterally as a neutrally buoyant gravity current, is known to depend on the properties (e.g., mass flux, thermal flux, volatile and external water content of the magma) at the vent and environmental conditions[9]. Volcanic plumes that entrain external water can be especially buoyant and high-reaching because of the added buoyancy from water vapor, especially from the latent heat released from water vapor condensation as the plume rises[10].

Critically, the 15 January 2022 HTHH eruption occurred after an approximately month-long period of eruptive activity that started on 19 December 2021 and that included two umbrella cloud producing eruptions. Here we assess the maximum heights and volume fluxes of the umbrella clouds from these recent eruptive phases of the HTHH (specifically, the explosive eruptions on 19 Dec 2021, 13 Jan 2022, and 15 Jan 2022). We focus on the umbrella cloud because it contains a significant fraction of volcanic material hours after eruption onset[11,12], is essential for understanding the physical processes associated with the HTHH explosive eruptions, and its behavior is likely correlatable with other data sets (e.g., seismic, atmospheric, infrasound, hydroacoustic, lightning[1,5,6]). We acknowledge that plumes often overshoot the umbrella cloud height and thus the umbrella height is not the maximum plume height. The plume overshoot height has been well-documented for the 15 January 2022 HTHH eruption at 55-58 km[7,8]. However, for analysis of the large-scale dispersal of material from an eruption, the umbrella cloud height can be a more representative height compared to the maximum plume height, which can be very transient and hence dependent on time resolution of the satellite datasets. Quantification of umbrella cloud height is also important for constraining plume models and, to our knowledge, has not been carefully analyzed to date for HTHH or similar submarine eruptions [1,11,12,13,14,15]. Quantifying volcanic cloud properties is a first step towards understanding the physical and dynamical processes that led to such a remarkably explosive eruption on 15 January 2022. Additionally, by evaluating this full eruptive sequence, we can put the 15 Jan 2022 eruption in context and lay the groundwork for understanding why the preceding HTHH submarine eruptions were not as explosive.

We used the full disk data of Himawari-8 geostationary satellite[16,17] (10-min temporal resolution and ~2 km pixel resolution at 11.2μm) to track the brightness temperatures (that is, the equivalent blackbody temperature) of the umbrella clouds through time. The overshooting top or pulses of plumes starts cooling down as it rises in the atmosphere, making the occurrence of overshoot detectable by assessing the minimum brightness temperature in an umbrella. We measure the minimum value of brightness temperature at the wavelength of 11.2μm ($BT_{11.2\mu m}$) within the umbrellas to infer when the plume produces overshooting tops. We also used the $BT_{11.2\mu m}$ to extract umbrella clouds' average temperature using a histogram and image segmentation[18] techniques (referred as BT_{Hist}) (see Methods). The histogram and image segmentation[18] techniques classify the pixels associated with umbrella clouds well. In contrast, averaging brightness temperature over a spatial fixed domain induces biases by both excluding portions of large umbrella clouds and including clear-sky pixels in evaluation of small umbrella clouds. To determine the umbrella cloud top heights from brightness temperature, we use the "temperature method"[19,20,21], which assumes that the umbrella clouds are in thermal equilibrium with their surroundings (see Methods). This temperature method primarily utilizes the real-time ECMWF Reanalysis version-5 (ERA5)[22] data.

Based on the above image segmentation and histogram techniques, we evaluate the area covered by umbrella clouds and measure the radial expansion of umbrella clouds as a function of time to calculate the volumetric flow rate (VFR) of the umbrella clouds[11,12] (see Methods). We calculate VFR for the initiation of each umbrella cloud (within the first 1–2 hours) and for the distinct eruptions during December 2021 and January 2022. The VFR and radial expansion patterns show how far and fast volcanic material (e.g., ash and water) was distributed near the neutral buoyancy levels.

For assessing the umbrella's composition and umbrella phase, we conducted a multi-channel analysis using channels 8.6µm, 11.2µm and 12.4µm[23,24,25,26,27] (see Methods) and various RGBs. With these tri-spectral channels and various RGBs, we primarily focus on the first order phase and optical properties of umbrella clouds (see Methods). A detailed investigation of ash detection using a combination of visible and thermal channels and radiative transfer modeling is out of the scope of this study.

Our results compare the umbrella cloud characteristics for three main events during recent HTHH eruptions between 19 Dec 2021 and 15 Jan 2022. These three major events are:

a. Initial eruption (19–20 Dec 2021)
b. Major eruption (13–14 Jan 2022)
c. Climactic eruption (15 Jan 2022)

Results

a. Initial eruption on 19 Dec 2021

The recent eruptive phase of HTHH began on 19 Dec 2021 at 20:40 UTC (see Movie S1, S2), shortly after which the altitude of an umbrella cloud reached around 15 km (with an uncertainty of 1–2 km; Figure 1e). The umbrella height was sustained for ~6 hours and this initial eruption subsided on 20 Dec 2021 between 01:00–02:00 UTC (see Movie S1). The umbrella cloud from this event laterally spread in the northeastward direction, due to prevailing westerly (eastward) wind in the upper troposphere (as identified from ERA5[22]) and covered an area of around 21 thousand square km within the first 150 min at contour level 220K (Figure 2a). Using this umbrella cloud area over the first 150 minutes of the eruption on 19 Dec 2021, and assuming spreading at the level of neutral buoyancy[11,12], the VFR was found to be $(3.7 \pm 0.7) \times 10^9$ m^3s^{-1} (Figure 2a). This VFR uncertainty is primarily linked to errors involved in analyzing the areal extent of umbrella clouds due to changes in the geolocation accuracy of the Himawari-8 pixels[28,29] and the natural variability of the Brunt-Väisälä frequency over tropics[30].

The brown color of the umbrella cloud in "ash RGB" (Figure 3b and Movie S3) and near zero values of $BTD_{11.2\text{-}12.4\mu m}$ (Figure 3c) indicate that most of the umbrella cloud was optically thick. However, the edge of umbrella clouds shows strong positive values of the $BTD_{8.6\text{-}11.2\mu m}$ and $BTD_{11.2\text{-}12.4\mu m}$, (Figure 3c, d and Movie S4, S5) suggesting optically thin ice clouds along the edge. The noticeable black/blue color near the outer edge of the umbrella in ash RGB (Figure 3b and Movie S3) confirms that this umbrella cloud contained a thin ice cloud. We cannot directly detect ash in the umbrella cloud because for an optically thick cloud in a humid environment, simple 2-channel and 3-channel BTD tests are limited for ash detection[26,27] (including the detection of ash embedded in the ice clouds). The ground-based observations of ash deposition across Tonga indicate that the umbrella cloud did have some ash component[31]. Overall umbrella cloud on 19 December 2021 was optically thick and contained significant ice.

We observed sporadic explosive eruptions between 20th and 31st Dec 2021 (see Movie S6) that produced plumes reaching 8–12km (Figure S1g) but no umbrella clouds. During this period, we observe intermittent fluctuations in $BT_{11.2\mu m}$ around the volcano (Figure S1e) indicative of sporadic eruptive activity. This shows a good agreement with a report by the Global Volcanism Program[31]. The prevailing meteorological clouds near the eruption site during 01–12 Jan 2022 hindered clear observations of brightness temperature changes related to volcanic activity. However, we do not see evidence for eruptions that surpassed the different meteorological clouds during this time. During occasional cloud-free conditions on 7th Jan, 11th Jan, and 12th Jan 2022, we observed intermittent weak pulses of $BT_{11.2\mu m}$ emanating from the eruption sites (see Movie S6).

b. Major eruption on 13 Jan 2022

With the clearing of the meteorological clouds, we could use Himawari-8 to observe a major eruption on 13 Jan 2022, starting around 15:20 UTC (see the first pulse around the HTHH vent in Movie S1). The altitude of the umbrella cloud top reached 18 km (with an uncertainty of 1–2 km), slightly crossing the tropopause height (Figure 1f). During 13-14 Jan 2022, the umbrella cloud was sustained near tropopause height for more than 22 hours, making this the longest-lived umbrella cloud of all three eruptions. We see evidence that the 13–14 Jan 2022 eruption was unsteady from fluctuations in BT_{min}, which indicates when plume overshoot occurred (Figure 1f; light-blue line). The lowest BT_{min} value was around 174.5K at 23:30 UTC, mid-way through the 13–14 Jan eruption. Compared to the BT_{min} fluctuations in 19–20 Dec 2021, this major eruption produced frequent fluctuations in BT_{min}, suggesting the occurrence of multiple explosions and an unsteady eruption.

The Jan 13–14 2022 volcanic cloud spread in the north-eastward direction following the upper tropospheric eastward moving wind (Movie S1). The umbrella clouds covered an area of about 30 thousand square km within the first 150 min (Figure 2b). For the initial 150 min of eruption on 13 Jan 2022, our estimation of VFR at contour level of 200K was found to be $(5.1 \pm 1.0) \times 10^9\ m^3s^{-1}$ (Figure 2b). The VFR on 13 Jan 2022 is almost 30% higher than the corresponding value on 19 Dec 2021.

On 13 Jan at 19:00 UTC, the bright white color in "true-color RGB" and brown color in "ash RGB" indicate the presence of high thick ice clouds (Figure 3f, g and Movie S2, S3). Similar to the 19 Dec, the black and dark blue colors in ash RGB (Figure 3g) indicate the thin ice cloud near the umbrella's edge. The positive magnitude of $BTD_{8.6\text{-}11.2\mu m}$ further confirms that the umbrella cloud exhibits an ice phase on 13 Jan 2022 (Figure 3i and Movie S5). The boundary between the near-zero $BTD_{11.2\text{-}12.4\mu m}$ and positive $BTD_{11.2\text{-}12.4\mu m}$ highlights the optical characteristics of these umbrella clouds.

As stated above, in an optically thick cloud over a humid environment, the ash detection is limited using thermal channels[26,27], and hence, we cannot determine the presence or absence of ash using the simple BTD tests. The local report from Tonga Geological Services confirmed ashfall over Tongatapu and Ha'apai group near Tonga island[32], suggesting that the umbrella cloud did have some ash particles. Overall, during the major eruption between 13-14 Jan 2022, the multi-channel analysis and true color/ash RGB suggest that the umbrella clouds contained significant ice content.

c. Climactic eruption on 15 Jan 2022

The climactic stage of the eruption began on 15 January 2022 shortly after 04:00 UTC, as seen from the reflectance satellite imagery (see Movie S2). We find that the umbrella cloud had an initial height of 31 km (with an uncertainty of 1–3 km), which is less than the overshoot height of around 55-58 km[7,8]. The average umbrella cloud height declines to 17 km (with an uncertainty of 1-2 km) over a period of ~11 hours (Figure 1g). During this period, the near-zero magnitude of $BTD_{11.2\text{-}12.4\mu m}$ shows that the umbrella clouds are optically thick except near the edge of the umbrella (see Movie S4).

The occurrence of plume overshoot time can be identified using BT_{min} values near the vent site. Any colder pixels near the vent site relative to the surrounding in the upper troposphere could indicate the start of an eruption or eruptive pluses. For example, the BT_{min} value near eruption initiation (04:20 UTC) was 170.93K in Himawari-8 10-min full disk data, colder than any point in the upper troposphere (Figure 1e-g). We identify a second instance of plume overshoot between ~08:30–08:40 UTC, as shown by a second decline in BT_{min} with a value of 181.19K (indicated by the light blue line in Figure 1g). We interpret the second overshoot to indicate a second eruptive pulse. One-min GOES-17[33] mesoscale observations were carried out over Tonga island, starting on 15 Jan 2022 at 07:05 UTC. At finer time-resolution, 1-min GOES-17 confirms the second dip at ~08:42 with a more precise minima value of 167.98K.

Two umbrella clouds and Volumetric Flow Rate (VFR)

We identify a second lower-altitude (17 km $\pm$ 1–2km, near the tropopause height) umbrella cloud that becomes visible at 05:30 UTC as the upper umbrella cloud moves westward, presumably due to advection by stratospheric winds (Figure 1d and see Movie S8). The lower umbrella cloud, U_A, has a distinct brightness temperature relative to the upper umbrella cloud: U_A ($BT_{11.2\mu m}$ < 210 K) and U_B (215K < $BT_{11.2\mu m}$ < 235K) (Figure 1d; indicated by two contour labels). At 05:00 UTC (Figure 2d), 1 hour after eruption onset, the frequency histogram of $BT_{11.2\mu m}$ is mainly dominated by U_B with a peak at ~230K. Starting around 05:30 UTC when the upper umbrella cloud moves westward, both U_A and U_B are identifiable in the time-series of frequency histogram of $BT_{11.2\mu m}$ (see Figure 2e and Movie S7, S8). Subsequently, by 11:50 UTC

(Figure 2f), the upper umbrella (U_B) has largely dissipated, and the frequency histogram shows the presence of the lower umbrella cloud, U_A.

The upper umbrella, U_B, expanded rapidly and covered an area of about 170 thousand square km, an area the size of Cambodia or Uruguay, within the initial 150 min (Figure 2c). The area covered by umbrella cloud during 19 Dec 2021 and 13 Jan 2022 is 13% and 17% of the areal coverage by U_B on 15 Jan 2022, respectively, for the same initial 150 min.

The satellite-based VFR for the upper umbrella cloud, U_B (contour levels between 215 and 235 K), is estimated to be $(5.0 \pm 1.0) \times 10^{11}$ $m^3 s^{-1}$ for the initial 50 min of eruption. The estimated VFR for the upper umbrella on 15 Jan 2022 is two orders of magnitude higher than the corresponding VFRs on 19 Dec 2021 and 13 Jan 2022, suggesting a much higher eruptive flux. We do not estimate a VFR for the lower umbrella because it was shielded by U_B and therefore not visible in its initial stages.

Composition of upper (U_B) and lower umbrella (U_A) clouds

On 15 Jan 2022, at 04:50 UTC, the true-color RGB shows the upper umbrella cloud in grey and white (Figure 3k, S2). The shadow marking on the northwestward umbrella edge suggests that it is a tall umbrella cloud (Figure 3k, S2). The overshooting plume is also visible in the true-color imagery at 04:50 UTC. The brown circular pattern in ash RGB also indicates the umbrella clouds are high-level thick clouds (Figure 3l). This is further discernable from near-zero magnitudes of $BTD_{11.2\text{-}12.4\mu m}$ and $BTD_{8.6\text{-}11.2\mu m}$ (Figure 3m, n and Movie S4, S5). The blue and black outer rim of U_B in the ash RGB (Figure 3l) indicates optically thin ice clouds along the edges of the umbrella. This is in qualitative agreement with the areas of blue boundaries near the outer rim of U_B in the maps of $BTD_{11.2\text{-}12.4\mu m}$ (Figure 3m and Movie S4) and $BTD_{8.6\text{-}11.2\mu m}$ (Figure 3n and Movie S5). Based on the observations from visible and thermal channels, we found that the upper umbrella, U_B, contains substantial ice.

The lower umbrella cloud, U_A, is also composed of abundant water and ice at 08:40 UTC, as indicated from the ash RGB and BTD tests. The widespread near-zero value of $BTD_{11.2\text{-}12.4\mu m}$

across the eruption site confirms that the U_A is optically thick. Some of the outer portions of U_A exhibit strong positive values of $BTD_{11.2\text{-}12.4\mu m}$, indicating the optically thin ice clouds. Overall, multi-channel analysis shows that most U_B and U_A areas are composed of optically thick ice clouds that have optically thin edges. The assessment of volcanic ash within the U_B and U_A could not be conducted due to limited ability of thermal channels to detect volcanic ash in optically thick ice clouds and a humid environment[26]. We expect, however, that at least the lower umbrella contained volcanic ash due to the widespread fallout of ash over the Kingdom of Tonga[31].

Discussion and Conclusions:

The 15 January 2022 eruption of HTHH was preceded by approximately a month of volcanic activity including two eruptions that produced umbrella clouds that spread along the tropopause. Our major findings are summarized below (see Figure 4, highlighting major findings):

1. The initial eruption occurred on 19 Dec at around 20:40 UTC for about 6 hours until 20 Dec 2021 between 01:00-02:00 UTC; the umbrella clouds reached an altitude of around 15 km $\pm$ 1–2 km and crossed slightly into the lower stratosphere. The satellite-based VFR for the Dec 19 event was $(3.7 \pm 0.7) \times 10^9\ m^3s^{-1}$. The volcanic umbrella clouds in the initial eruption on 19 Dec were mainly made of thick ice clouds. Between late Dec 20 and 31 Dec 2021, we observed the production of weak plumes that reached 8-12 km. During 01-12 Jan 2022, we did not observe volcanic plumes as meteorological clouds may have hindered the ability to interpret small plumes. During cloud-free conditions on 7th Jan, 11th Jan, and 12th Jan 2022, we observed intermittent weak pulses of $BT_{11.2\mu m}$ emanating from the vent.

2. A major eruption started on 13 Jan 2022 at 15:20 UTC and was sustained for about 22 hours, making this the longest lasting umbrella studied here. The umbrella cloud reached an altitude of 18 km $\pm$ 1–2 km and the initial VFR was $(5.0 \pm 1.0) \times 10^9 m^3s^{-1}$. Significant fluctuations in the minimum brightness temperature values suggest that the eruption was unsteady with many intermittent eruptive pulses. Similar to 19 Dec

2021, the 13 Jan 2022 umbrella had significant ice content and was made of optically thick high-level ice clouds.

3. On 15 Jan 2022, the Himawari-8 reflectance data captured the start of the eruption at approximately 04:00 UTC. An (upper) umbrella cloud developed quickly and obtained an area of 112 thousand km^2 within 50 mins. The initial satellite-derived VFR for the upper umbrella cloud on 15 Jan 2022 was $(5.0 \pm 1.0) \times 10^{11}\ m^3s^{-1}$, nearly two orders of magnitude higher than that estimated on 19 Dec 2021 and 13 Jan 2022 eruptions. We identified two distinct umbrella clouds at two different altitudes: an upper umbrella U_A that spread in the stratosphere at 31 km $\pm$ 1–3km and a lower umbrella cloud that spread at the tropopause at 17 km $\pm$ 1–2km. The lower cloud, U_A, only became visible an hour and a half after eruption onset at 05:30 UTC as the upper umbrella cloud was advected westward, presumably due to the easterly wind in the stratosphere near 30 hPa.

4. We observed a second eruptive pulse at ~08:40 UTC, four hours after the start of the eruption, that produced plume overshoot. This was inferred from the coldest $BT_{11.2\mu m}$ occurring at 08:40 UTC with a value of 181 K. We found that both U_B and U_A were made of thick ice clouds but could not resolve the presence or absence of ash. Thick layer of ashfall were reported during climactic eruption[1], which implies that these umbrella clouds did comprise some ash particles.

Results on the timelines of overshooting volcanic plumes (based on BT_{min}) and umbrella heights (based on BT_{Hist}) provide foundational data for plume models[34,35] and reveal important eruption features that compare well against other independent data sets. For example, we identified a second eruptive pulse on 15 Jan 2022 that produced plume overshoot at ~08:40 UTC – an aspect of the eruption sequence not yet recognized using satellite remote sensing. Analysis of infrasound and hydroacoustic stations revealed a final eruptive pulse at ~08:31 UTC on 15 Jan 2022[5], consistent with the timing of the second plume overshoot. Together these observations lead to questions about the causes of these two eruptive pulses. In this context, one of the goals of this study is to provide a foundational timeline against which other future data sets[5,36] (e.g., seismic) can be compared to build a more complete picture of eruptive processes.

The VFRs associated with the HTTH eruptions on 19 Dec 2021 and 13 Jan 2022 qualitatively agree (with the uncertainty limit) with the explosive submarine eruption of Anak Krakatau[28] on 22 Dec 2018 (~5×10^9 m^3s^{-1}).

The 15 Jan 2022 HTHH eruption is unlike previously documented eruptions because of its double umbrella cloud (e.g., U_A and U_B at 18 and 31 km, respectively). Although multiple neutral buoyancy layers have been observed for multi-phase fluid plumes (e.g., Deepwater Horizon hydrocarbon plume with oil and as bubbles[37], various lab experiments[38]), this phenomenon has not been documented for volcanic eruptions with extensive umbrellas to the best of our knowledge[39]. Furthermore, 3D numerical volcanic plume models for subaerial eruptions also do not have the multiple umbrella cloud features. We hypothesize that the water-rich nature of the HTHH eruption may have facilitated the development of the double umbrella, possibly due to extensive ice condensation and latent heat driven processes making the volcanic plume more akin to strongly multiphase buoyant plume. However, at this point the specific mechanisms that drove double umbrella formation are not known and require future work.

The 15 Jan 2022 HTHH eruption shares several features with the 1991 eruption of Mount Pinatubo. Both eruptions produced plume overshoot and umbrella clouds (plume top height was at ~37 km and umbrella top height was at ~25km for the climactic stage of Pinatubo[15,39]) and similar eruption duration. The average VFR during the 15 June 1991 climactic eruption of Pinatubo was around one order lowered (5.8–7 x 10^{10} m^3s^{-1}; Figure 2e) than the recent 15 January 2022 climactic eruption of HTHH[15,39]. That said, the 15 Jan HTHH produced higher plume and upper umbrella cloud top heights (~55 km and ~31 km, respectively) compared to Pinatubo. Next, we compare their ratios of umbrella top heights to plume top heights. The 15 Jan 2022 HTHH eruption had an umbrella to plume top height ratio of 0.58, less than 1991 Pinatubo's ratio of 0.68 (and Calbuco 2015's 0.71 and Kelud 2014's 0.71)[15]. This comparison shows that HTHH's plume was exceptionally high reaching, even for an eruption that created an umbrella at ~31 km and highlights the potential influence of enhanced water associated buoyancy. Since the characteristics of the HTHH eruption are different from other subarerial eruptions, we do not attempt to use the plume or the umbrella height to estimate a mass eruption rate since these relationships have not explicitly been calibrated for large submarine eruptions.

Our findings of the abundant water and ice content on 15 Jan 2022 qualitatively agree with the reporting by Millan[41] and Xu [42] (using Aura Microwave Limb Sounder data) that the eruption added an unprecedented (>10% of the total stratospheric H_2O burden) amount of water to the stratosphere compared to any eruption or wildfire over the past 2 decades. The primary stratospheric hydration close to the eruption was observed at ~20–10 hPa (~25–31 km) levels, consistent with being sourced from the dominant upper HTHH Umbrella cloud (U_B).

Additionally, Kloss[43] (using in-situ balloon-borne observations of the plume at La Reunion island) found that the Hunga Tonga plume one week after the eruption had no coarse (> 1 μm) ash aerosol component in contrast with Pinatubo 1991 or the Raikoke 2019 eruption[44]. This balloon-borne result is to first order, consistent with our observation of a lack of strong ash signature in the umbrella cloud although there are significant uncertainties in the eruption's initial ash content due to the possibility of ice coated ash particles and rapid ash sedimentation after the eruption.

The global dispersal of the umbrella cloud, with abundant water and ice content in the stratosphere region, could strongly influence the longwave and solar radiations at the top-of-the-atmosphere (TOA), which can, in turn, regulate the Earth's surface temperature and climate. Sellitto[45] showed that immediately after the eruption, the longwave (LW) water vapor cooling dominates the umbrella cloud's localized stratospheric in-plume heating/cooling rates and produces a rapid descent of the umbrella (qualitatively consistent with our umbrella cloud height measurements). Over the longer term, three-four weeks after the climactic eruption, Sellitto[45] showed that the water vapor's TOA radiative forcing switches sign (due to decreased altitude) and is +0.8 Wm^{-2}, thus canceling out the cooling impact of aerosols[45]). For comparison, the aged plume TOA for large recent volcanic eruptions (e.g., Raikoke 2019, Ambae 2018) and wildfires (e.g., Australian bushfires 2019–2020), as well as the Pinatubo 1991 eruption[46,47], are typically negative with values ranging from -3.5 (Pinatubo) to -0.3 Wm^{-2}.

Methods

Extraction of umbrella clouds

Before estimating volcanic umbrella top height, it is important to accurately assess the magnitude of $BT_{11.2\mu m}$ related to the umbrella top. To do this we average $BT_{11.2\mu m}$ values (also estimate the standard deviation) from all pixels associated with the umbrella clouds. Defining the pixels (area) associated with the umbrella clouds is challenging, however, because umbrella cloud areas evolve as the clouds grow, shrink, and are advected by winds. For example, if one were to consider all $BT_{11.2\mu m}$ values in an eruptive area, the non-volcanic clouds overpassing near the eruption site and clear-sky conditions are likely to affect the above magnitude of $BT_{11.2\mu m}$. Other factors, such as semi-transparent clouds and high overshooting cloud top, can bias the $BT_{11.2\mu m}$ towards colder temperatures in the troposphere and warmer temperatures in the stratosphere. However, over a large number of measurements, these biases should be reduced when the umbrella cloud covers the majority of a given area. For a large sample of measurements near HTHH eruption sites, we developed a histogram and image segmentation method for evaluating the $BT_{11.2\mu m}$ associated with the umbrella clouds. This histogram method for extraction of umbrella clouds is primarily based on the image segmentation technique[18]. After assessing the $BT_{11.2\mu m}$ values for a given umbrella cloud and verifying that the umbrella clouds are optically thick and in thermal equilibrium with the surrounding, we can retrieve the top heights of umbrella clouds using ERA5 temperature profiles[19,20,21,22].

Histogram and image segmentation technique—BT_{Hist}:

To determine a brightness temperature that captures the umbrella cloud top border, we determine the frequency of occurrence of $BT_{11.2\mu m}$ over a large sample of measurements covering an area as shown in Figure 1a-d and Movie S7 (2000 pixels x 1245 pixels areas; each pixel has ~2 km resolution for thermal channels; although pixel resolution changes with the solar zenith angle[16,17]).

The $BT_{11.2\mu m}$ magnitudes in Figure 1a-d may correspond to volcanic, non-volcanic clouds or clear-sky conditions. In a clear-sky condition, the frequency of occurrence of $BT_{11.2\mu m}$ should peak at near-surface temperature. Similarly, suppose umbrella clouds are present as exemplified in Figure 1a-d. In that case, the frequency histogram of $BT_{11.2\mu m}$ (when warmer pixels > 270K are removed to avoid biasing towards clear pixels) should be high near a temperature, reasonably representing a peak temperature value (referred as T_{peak}) associated with the umbrella clouds. In a given image (e.g., Figure 1a-d), the T_{peak} will also encompass the interior region of the umbrella cloud during the initial growth phase. For all three umbrella formation events (that is, 19 Dec 2021, 13 Jan 2022, 15 Jan 2022), the T_{peak} associated with each umbrella cloud may be different. For a given eruption, we take the upper bound of T_{peak} in such a way that we incorporate maximum possible umbrella features and avoid any non-volcanic cloud influences. For instance, for the 19 Dec 2021 eruption, a threshold value (T_U) of contour level was determined based on the time-varying loops of T_{peak} and its upper bound at which the umbrella is not influenced by non-volcanic clouds surrounding the volcanic umbrella regions. For all three events, the upper bound is generally bounded within 5K to 12K of T_{peak}. We referred to this upper bound of T_{peak} as threshold value (T_U) associated with umbrella clouds. Therefore, the selection of contour level T_U depends upon the peak frequency histogram of brightness temperature of umbrella clouds. After finding the umbrella threshold temperature, T_U < 220K for 19-20 Dec 2021 (initial eruption), T_U < 210K for 13-14 Jan 2022 (major eruption), 215K < T_{UB} < 235K for the upper umbrella on 15 Jan 2022 (climactic eruption), T_{UA} < 210 K for the lower umbrella on 15 Jan 2022 (climactic eruption), we then followed a set of procedures to estimate the mean $BT_{11.2\mu m}$ (including standard deviation) of these umbrella clouds (see Fig. 3e, j, o, t and Movie S8):

1. We first apply threshold temperature conditions defined above on the $BT_{11.2\mu m}$ map (shown in Figure 1a-d). This enables removing some of the warmer pixels associated with clear-sky or non-volcanic clouds, as stated above. We then create a bi-level image of $BT_{11.2\mu m}$ with 0s (pixels not satisfying the threshold temperature condition) and 1s (pixels satisfying the threshold temperature condition).

2. In the bi-level image obtained from point (1), we perform a maximum frequency histogram test on all the "1s" to make sure that the pixels reasonably represent the umbrella clouds. After finding all indices of pixels associated with umbrella clouds, we extracted the $BT_{11.2\mu m}$ magnitudes associated with umbrella clouds. The extracted

umbrellas using point (1) and (2) are shown in Figure 3e, j, o, t (see supplementary Movie S8 for 15 Jan 2022).

3. We then calculate the conditional mean and standard deviation of these $BT_{11.2\mu m}$ pixels associated with umbrella clouds using point (1) and (2). Subsequently, we create a time-series of the mean and standard deviation of $BT_{11.2\mu m}$ (defined as BT_{Hist} in Fig. 1e-g).

4. Furthermore, using point (2), we mapped the indices associated with the umbrella clouds over latitude/longitude area and evaluated the total areal and radial extents covered by umbrella clouds (Fig. 2a-c).

After obtaining BT_{Hist}, we use the temperature method (described below) to estimate the height of these umbrella clouds. The uncertainty in the umbrella height is determined using the uncertainty in the BT_{Hist} values. But before estimating the umbrella height, we assessed the optical properties of these umbrella clouds based on the $BTD_{11.2\text{-}12.4\mu m}$ values. For instance, if $BTD_{11.2\text{-}12.4\mu m}$ is close to zero, it most likely represents an optically thick cloud.

Estimation of umbrella cloud height

To convert brightness temperature to height, we determined the altitude at which the brightness temperature was equivalent to the atmospheric temperature using real-time ERA5[22] atmospheric profile data, which provides hourly estimates of real-time pressure level data, such as atmospheric temperature, vertical pressure, and vertical velocity.

Temperature method—H_U (Umbrella top height)

For evaluating umbrella heights, we match the satellite's estimated BT_{Hist} with the collocated and linearly interpolated ERA5[22] temperature profile in real-time. This conversion method of brightness temperature value to vertical height using the ERA5 temperature profile is called the "temperature method"[19,20,21]. As stated above, this method is especially useful for optically thick umbrella clouds when they are in thermal equilibrium with the surrounding environments. The assumptions inherent in this conversion are: (1) the umbrella cloud is optically thick so that the thermal emission is primarily associated with the uppermost cloud top layer, and (2) the umbrella cloud is not influenced by the non-volcanic cloud and clear-sky pixel temperatures. The above assumptions imply that the temperature method is applicable when the umbrella cloud's brightness temperature is in thermal equilibrium with its ambient environment. To test assumption (1), that the umbrella clouds are optically thick, we apply the near-zero difference test between brightness temperature at 11.2μm and 12.4μm and find that the umbrellas are optically thick everywhere except their outermost edges. For testing assumption (2), our histogram techniques avoid the influence of non-volcanic clouds and clear-sky pixel temperatures.

Umbrellas reaching either the troposphere or the stratosphere can have two height solutions based on the ERA5 temperature profiles. Still, only one of the heights will be a true solution for the plume falling in the stratosphere or troposphere. We can find this true solution based on the time-varying $BT_{11.2\mu m}$ associated with umbrella clouds. For instance, in an explosive eruption, if plume overshoots into the stratosphere and umbrella clouds are initially lying in the stratosphere, they will remain stratospheric and eventually spread along with a neutral buoyancy level in the stratosphere for a certain duration. In this case (e.g., on 15 Jan 2022), the correct height solution should be taken from the ERA5 temperature profile in the stratosphere. Based on the a priori information of the time series of the brightness temperature of the volcanic cloud and the ERA5 temperature profile, we can select the correct height solution and also estimate the associated uncertainty values.

However, when an eruption is weak and the plume breaks in the middle atmosphere without an umbrella formation, the ERA5 temperature method may yield an ambiguous solution. Moreover, the ERA5 temperature-based height-retrievals are not applicable when an eruption produces overshooting cloud tops. The overshooting cloud tops related to volcanic eruptions could reach into the stratosphere, causing the breakdown of the hydrostatic equilibrium state. In this scenario, the assessment of overshooting top height using the ERA5 temperature method will not be applicable or produce ambiguous results and one needs to apply other techniques, such as stereoscopic[7,8], shadow trigonometry[21]. Consequently, our analysis in this study has focused exclusively on the umbrella clouds which satisfy the requirements for the temperature methods.

For two overpasses of CALIPSO datasets[48] on 14 Jan 2022 at 14:27 UTC (over 179.17ºE, 21.70ºS) and 16 Jan 2022 at 15:42 (over 160.02ºE, 22.68ºS), we find that the altitude of a strong total attenuated backscatter signal at 532 nm from 18 km and 32 km, respectively. This total attenuated backscatter signal at 532 nm is primarily related to the stratospheric aerosol layer and volcanic clouds. Since the lifetime of the stratospheric aerosol layer is high, it is reasonable to assume the umbrella cloud has also attained a similar altitude (Fig. S3 and S4). The CALIPSO estimated heights are consistent with our measured umbrella heights and thus help validate the accuracy of our method.

Differentiating U_A and U_B

The frequency histogram over 2000 pixels x 1245 pixels areas in Figure 1d give a priori information to characterize umbrella clouds. We also evaluate the frequency histogram of $BT_{11.2\mu m}$ as a function of time for the above domain to characterize the peak $BT_{11.2\mu m}$ for U_A and U_B. The time series of frequency histograms of $BT_{11.2\mu m}$ associated with U_B shows that this peak varies between ~235K and ~215K (see Movie S7). Thus, the upper umbrella was characterized for $215K < BT_{11.2\mu m} < 235K$. Similarly, lower tropospheric umbrella U_A was characterized.

Volumetric Flow Rate Estimates

Using point (4) of histogram technique (see above), we determined the time-series of areal extents (A) of umbrella clouds which is then converted into radial extent (R), using $R = \sqrt{A/\pi}$ as the umbrella was elongated in one direction (eastward on 19 Dec 2021 and westward during other three events) due to prevailing wind in the upper troposphere and stratosphere. For estimating volumetric flow rate (VFR), we use the parameterization equation[11,12,13,14]

$R = \left({}^{3\lambda QN}/_{2\pi} \right)^{1/3} t^{2/3}$ (where λ is a constant that is approximately 0.2, Q is the volume flux and *N* is the Brunt-Väisälä frequency, and *t* is time) to fit with our measurements of spherical-equivalent plume top radius through time for the initial 50-150 min (Figure 2a-c). Also, the Brunt–Väisälä frequency (N) is taken as 0.026 near tropopause and 0.022 at around 30 km in the stratospheric region as evaluated using ERA5[22] reanalysis data. In estimating the VFR, we accounted for viewing zenith angle correction. The uncertainty in VFR can be attributed to errors involved in analyzing the areal extent of umbrella clouds from Himawari-8 pixels[16, 17], unsteadiness of the eruption, and because of the natural variability of the Brunt-Väisälä frequency over tropics[28]. The geolocation accuracy of Himawari-8/AHI is around 2km. The error in estimating the areal extent of umbrella clouds due to assumption of perfectly circular umbrella from Himawari-8 pixels is ~10% per 30km radius[28, 29]. The error with the natural variability of Brunt-Väisälä frequency is ~10%[30]. Moreover, above parameterization equation for the VFR estimation in a changing umbrella cloud with height may also produce some inaccuracy[11,12,13,14].

REFERENCES:

1. Global Volcanism Program. Report on Hunga Tonga-Hunga Ha'apai (Tonga). In: Sennert, S K (ed.), Weekly Volcanic Activity Report, 16 February-22 February 2022. Smithsonian Institution and US Geological Survey (2022).

2. Brenna, M. et al. Post-caldera volcanism reveals shallow priming of an intra-ocean arc andesitic caldera: Hunga volcano, Tonga, SW Pacific, Lithos, 412–413, 106614 (2022).

3. Yuen, D. A. et al. Under the surface: Pressure-induced planetary-scale waves, volcanic lightning, and gaseous clouds caused by the submarine eruption of Hunga Tonga-Hunga Ha'apai volcano. Earthquake Res. Adv., 100-134 (2022).

4. Wright, C. et al. Tonga eruption triggered waves propagating globally from surface to edge of space, Atmos. Sci., https://doi.org/10.1002/essoar.10510674.1, (2022).

5. Matoza, R. S. et al. Atmospheric waves and global seismoacoustic observations of the January 2022 Hunga eruption, Tonga, Science, eeeeeeeeeee. DOI:10.1126/science.abo7063 (2022).

6. Omira, R., Ramalho, R.S., Kim, J. et al. Global Tonga tsunami explained by a fast-moving atmospheric source. Nat., https://doi.org/10.1038/s41586-022-04926-4, (2022).

7. Carr, J.L., Horváth, Á., Wu, D.L. & Friberg, M.D. Stereo Plume Height and Motion Retrievals for the Record-Setting Hunga Tonga-Hunga Ha'apai Eruption of 15 January 2022. *Geophy. Res. Lett.*, *49*(9), e2022GL098131, (2022).

8. NASA Earth Observatory. Tonga Volcano Plume Reached the Mesosphere. (2022).

9. Carey, S. & Marcus B. "Volcanic plumes." In The encyclopedia of volcanoes, pp. 571-585. Academic Press, (2015).

10. Hanna, S. R. Rise and condensation of large cooling tower plumes. J. Appl. Meteoro. Climatolo., 11(5), 793-799, (1972).

11. Costa, A., Folch, A., & Macedonio, G. Density-driven transport in the umbrella region of volcanic clouds: implications for tephra dispersion models. Geophys. Res. Lett. 40, 4823–4827 (2013).

12. Woods, A. W. & Kienle, J. The dynamics and thermodynamics of volcanic clouds: Theory and observations from the april 15 and april 21, 1990 eruptions of redoubt volcano, Alaska. *J. Volcanol. Geotherm. Res.* 62, 273–299 (1994).

13. Sparks, R. The dimensions and dynamics of volcanic eruption columns. Bull. Volcanol., 48(1), 3-15 (1986).

14. Mastin, L.G. Testing the accuracy of a 1-D volcanic plume model in estimating mass eruption rate. Journal of Geophy. Res.: Atmos., 119(5), 2474-2495 (2014).

15. Webster, H.N., Devenish, B.J., Mastin, L.G., Thomson, D.J. & Van Eaton, A.R. Operational modelling of umbrella cloud growth in a lagrangian volcanic ash transport and dispersion model. Atmos., 11(2), 200 (2020).

16. Bessho, K. et al. An Introduction to Himawari-8/9–Japan's New-Generation Geostationary Meteorological Satellites. J. Meteorol. Soc. Jpn. Ser II 94, 151–183 (2016).

17. Suzuki, M., Taniguchi, H., Tsuchiyama, H., Uesawa, D., Yokota, H., and Yoshida, R.: An Introduction to Himawari-8/9–Japan's New-Generation Geostationary Meteorological Satellites, 94, 151–183 (2016).

18. Canty, M.J. Image analysis, classification and change detection in remote sensing: with algorithms for ENVI/IDL and Python. Crc Press (2014).

19. Prata, A. J., and I. F. Grant. "Retrieval of microphysical and morphological properties of volcanic ash plumes from satellite data: Application to Mt Ruapehu, New Zealand." Q. J. Royal Meteorol. Soc. 127, 576, 2153-2179 (2001).

20. Hamann, U. Remote sensing of cloud top pressure/height from SEVIRI: analysis of ten current retrieval algorithms. Atmos. Measurement Techniques, 7(9), 2839-2867 (2014).

21. Horváth, Á. et al., (2021). Geometric estimation of volcanic eruption column height from GOES-R near-limb imagery–Part 2: Case studies. Atmos. Chem. Phys., 21(16), 12207-12226 (2021).

22. Hersbach, H. et al. The ERA5 global reanalysis. Q. J. R. Meteorol. Soc. 146, 1999–2049 (2020).

23. Prata, A. J. "Observations of volcanic ash clouds in the 10-12 μm window using AVHRR/2 data." Int. J. Rem. Sens. 10(4-5): 751-761 (1989).

24. Prata, A. J. Infrared radiative transfer calculations for volcanic ash clouds. Geophys. Res. Lett. 16, 1293–1296 (1989).

25. Strabala, K. I., Ackerman, S. A., & Menzel, W. P. Cloud Properties inferred from 8–12-μm Data, J. Appl. Meteorol. Climatolo., 33(2), 212-229 (1994).

26. Rose, W.I. et al. Ice in the 1994 Rabaul eruption cloud: implications for volcano hazard and atmospheric effects. Nat., 375(6531), 477-479 (1995).

27. Prata, F., Bluth, G., Rose, B., Schneider, D., & Tupper, A.: Comments on "Failures in detecting volcanic ash from a satellite-based technique," 78, 341–346 (2001).

28. Prata, A. T. et al. Anak Krakatau triggers volcanic freezer in the upper troposphere. *Sci. Rep.* 10, 3584 (2020).

29. Takeuchi, W. Assessment of geometric errors of Advanced Himawari-8 Imager (AHI) over one year operation. In IOP Conference Series: Earth and Environmental Science, vol. 37(1) 012004. IOP Publishing (2016).

30. Wüst, S., Bittner, M., Yee, J. H., Mlynczak, M. G., & Russell III, J. M. Variability of the Brunt–Väisälä frequency at the OH∗-airglow layer height at low and midlatitudes. Atmos. Measur. Tech., 13(11), 6067-6093 (2020).

31. Global Volcanism Program. Report on Hunga Tonga-Hunga Ha'apai (Tonga) (Crafford, A.E., and Venzke, E., eds.). Bulletin of the Global Volcanism Network, 47:2. Smithsonian Institution (2022).

32. News report based on Tonga Geological Services, 51 Vaha'akolo Road, Nuku'alofa, Tonga, https://matangitonga.to/2022/01/14/volcanic-plume-ash-steam-and-gas-over-tonga, (2022).

33. Schmit, T. J. et al. A Closer Look at the ABI on the GOES-R Series, Bull. Am. Meteorol. Soc., 98(4), 681-698 (2017).

34. Costa, A., J Suzuki, Y., & Koyaguchi, T. Understanding the plume dynamics of explosive super-eruptions. *Nat. Commun., 9*(1), 1-6 (2018).

35. Mastin, L. G. A user-friendly one-dimensional model for wet volcanic plumes. Geochem. Geophys. Geosystems 8, (2007).

36. Fauria, K. E. et al. Simultaneous creation of a large vapor plume and pumice raft by a shallow submarine eruption, preprint, https://doi.org/10.1002/essoar.10510412.1, (2022).

37. Socolofsky, S.A., Adams, E.E. & Sherwood, C.R. Formation dynamics of subsurface hydrocarbon intrusions following the Deepwater Horizon blowout. Geophys. Res. Lett., 38(9) (2011).

38. Mingotti, N. & Woods, A.W. Multiphase plumes in a stratified ambient. J. Fluid Mechanics, 869, 292-312 (2019).

39. Mastin, L.G. & Van Eaton, A.R. Comparing Simulations of Umbrella-Cloud Growth and Ash Transport with Observations from Pinatubo, Kelud, and Calbuco Volcanoes. Atmos., 11(10), 10-38 (2020).

40. Holasek, R.E., Self, S. & Woods, A.W. Satellite observations and interpretation of the 1991 Mount Pinatubo eruption plumes. J. Geophys. Res.: Solid Earth, 101(B12), 27635-27655 (1996).

41. Millan, L. et al. The Hunga Tonga-Hunga Ha'apai Hydration of the Stratosphere, preprint, https://doi.org/10.1002/essoar.10511266.1, (2022).

42. Xu, J., Li, D., Bai, Z., Tao, M. & Bian, J. Large Amounts of Water Vapor Were Injected into the Stratosphere by the Hunga Tonga–Hunga Ha’apai Volcano Eruption. Atmosphere, 13(6), 912 (2022).

43. Kloss, C. et al. Aerosol characterization of the stratospheric plume from the volcanic eruption at Hunga Tonga January 15th 2022, preprint, https://doi.org/10.1002/essoar.10511312.1, (2022).

44. Kloss, C. et al. Stratospheric aerosol layer perturbation caused by the 2019 Raikoke and Ulawun eruptions and their radiative forcing. Atmos. Chem. Phys., 21(1), 535-560 (2021).

45. Sellitto, P. et al. The unexpected radiative impact of the Hunga Tonga eruption of January 15th, 2022 (2022).

46. Bergstrom, R.W., Kinne, S., Russell, P.B., Bauman, J. J. & Minnis, P. Radiative Forcing of the Pinatubo Aerosol as a Function of Latitude and Time (1996).

47. Kloss, C. et al. Impact of the 2018 Ambae eruption on the global stratospheric aerosol layer and climate. J. Geophys. Res.: Atmospheres, 125(14), e2020JD032410 (2020).

48. Winker, D. M., Hunt, W. H. & McGill, M. J. Initial performance assessment of CALIOP. *Geophys. Res. Lett.* 34, (2007).

49. EUMETSAT User Services. Best practices for RGB compositing of multi-spectral imagery. Darmstadt, (2009).

50. Miller, S. el al. A Sight for Sore Eyes - The Return of True Color to Geostationary Satellites. *Bull. Amer. Meteor. Soc.* (2016).

Acknowledgments: The Himawari-8 radiance data are obtained from the National Institute of Information and Communications Technology (NICT) Science Cloud, Japan. We thank John Rausch for his support in obtaining the Himawari-8 data.

Funding: This work was funded by National Aeronautics and Space Administration (NASA) grant 80NSSC20K1450 to PI (K.E.F) and Co-PI (R.B.). A.G. was supported with this funding. TM was supported by a Massachusetts Institute of Technology Crosby fellowship.

Author contributions:

AG analyzed the data and developed it with R. B., K. E. F., and T. M. A. G., R. B., K. E. F., and T. M. contributed to conceptual development of this work. K. E. F., R. B. and T. M. supervised this research. K. E. F. and R. B. obtained NASA funding. A. G. drafted the original manuscript. The manuscript was reviewed and edited by K. E. F, T. M., and R. B.

Competing interests: Authors declare that they have no competing interests.

Data and materials availability:

The Himawari-8 data used in this study are available in public domain and it can be also obtained from https://registry.opendata.aws/noaa-himawari/. Eight supplementary Movies and .csv file related to Figure 1e-g can be accessed using this link (https://zenodo.org/record/6757667).

Code availability:

All the images in a Figure 1, 2, and 3 (including Movies) are generated using Python 3 and open source matplotlib library (https://www.python.org/downloads/ & https://matplotlib.org/stable/index.html) and Himawari-8 data. Source code for extracting umbrella clouds is available upon request from A. K. G. or R. B.

Main Figures:

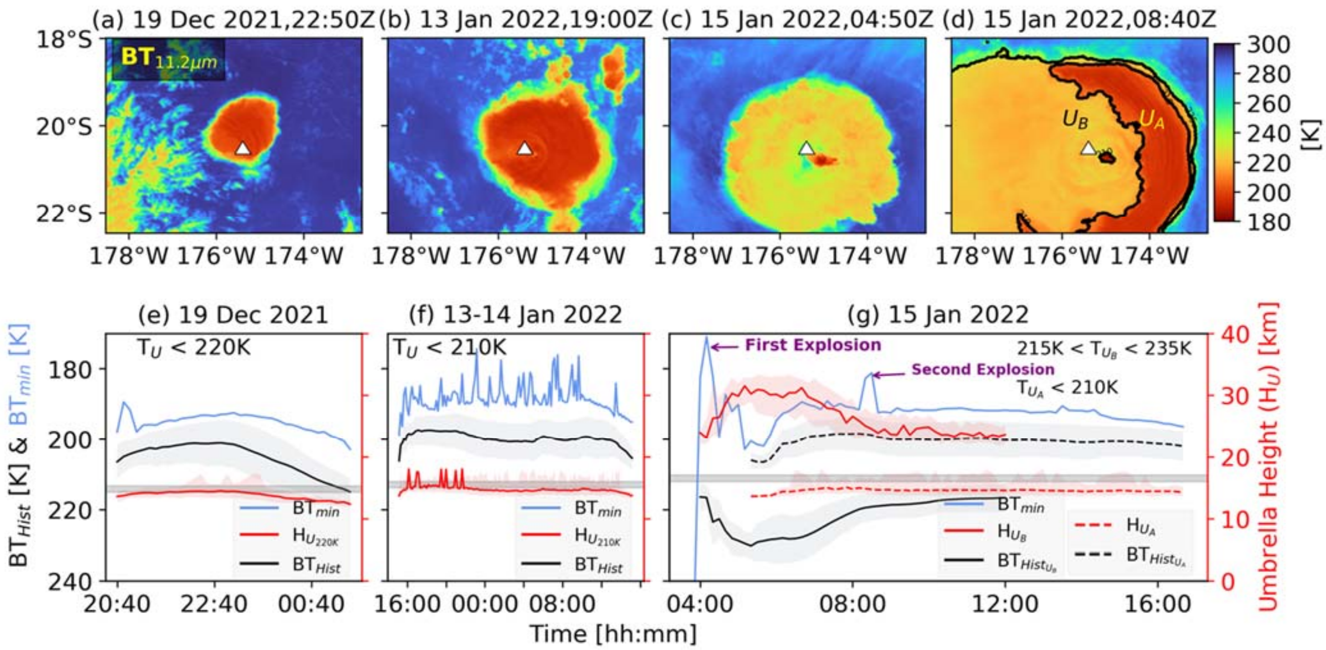

Figure 1: Upper panels: (a) Himawari-8 observed brightness temperature at 11.2 microns ($BT_{11.2\mu m}$) centered around Hunga Tonga-Hunga Ha'apai (HTHH) (175.38°W, 20.57°S) submarine volcano on 19 December 2021 at 22:50 UTC. Panel (b), (c) and (d) are similar to panel (a) but for 13 January 2022 at 19:00 UTC, 15 January 2022 at 04:50 UTC, 15 January 2022 at 08:40 UTC, respectively. Two contour levels in panel (d) indicate U_A and U_B (separated umbrella clouds). The contour U_A is outlined for $BT_{11.2\mu m}$ (T_{U_A}) < 210K, and contour U_B is outlined for 215K < $BT_{11.2\mu m}$ (T_{U_B}) < 235K. The colorbar represents the brightness temperature ($BT_{11.2\mu m}$) measured in Kelvin [K]. **Bottom panels**: (e) the black line (BT_{Hist} [K]) indicates a histogram of $BT_{11.2\mu m}$ associated with umbrella clouds at a contour level of 220 K during the HTHH eruptions on 19-20 December 2021 (initial eruption starting at 20:40Z on 19 December). The red line ($H_{U_{220K}}$) represents the umbrella height in km. The uncertainties associated with BT_{Hist} [K] and $H_{U_{220K}}$ are indicated using grey and light red shaded colors. The light blue line represents the minimum $BT_{11.2\mu m}$ (BT_{min}) covering the entire domain shown in the upper panel (a). The light grey horizontal bar around 16 km is the mean tropopause height during 19-20 December 2021. (f) Same as (e) but for 13-14 January 2022 (major eruption starting at ~15:20Z on 13 January). (g) On 15 January 2022, BT_{Hist} is shown for two distinct umbrella clouds:

BT_{HistU_A} (dashed red line) and BT_{HistU_B} (solid red line). The umbrella heights H_{U_A} and H_{U_B} are estimated for corresponding BT_{HistU_A} and BT_{HistU_A}. Again, the light blue line represents the minimum $BT_{11.2\mu m}$ (BT_{min}) covering the entire domain shown in upper panel (d). Two explosions on 15 January in the interval of four hours are marked by purple color arrows.

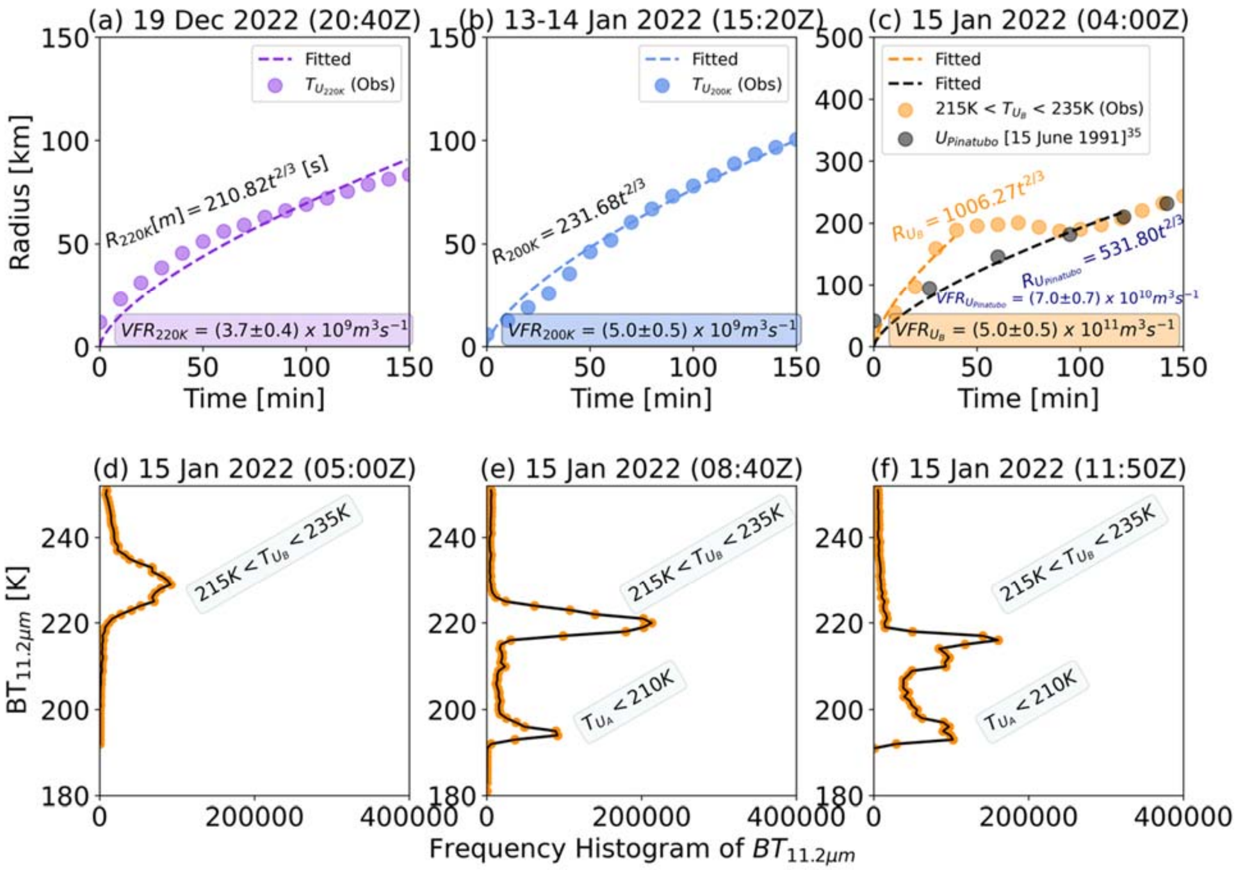

Figure 2: Upper panels: (a) On 19 December 2021 (initial eruption starts around 20:40 UTC), the radial change of umbrella height as a function of the initial 150 minutes is estimated using the Himawari-8 observations (Obs) and described by violet dots. The dashed purple line in panel (a) indicates the polynomial fitting for the initial 150 min for the contour labeled at 220 K. The R (in meter) and t (in sec) relations and volumetric flow rate (VFR) and associated uncertainty values are described by the inset text at different $BT_{11.2\mu m}$ contour levels. (b) Same as (a) but 13-14 January 2022 eruption time (starting at 15:20 UTC). In this case, the polynomial fitting is

performed for the 200K $BT_{11.2\mu m}$ value. The R and VFR represent the same as in (a). (c) Same as (a) but for the greatest explosive eruption on 15 January 2022 starting between 04:00-04:10 UTC (true color RGB shows the initial eruption at 04:00 UTC). In panel (c), the radial expansion of the umbrella with time during the climactic eruption of Pinatubo for the contour level between 220K and 240K was taken from Mastin[35]. **Bottom panels**: (d) On 15 January 2022 at 05:00 UTC, the frequency histogram of $BT_{11.2\mu m}$ was estimated for the entire area of Fig. 1d. At 05:00 UTC, the upper umbrella cloud (215 K < T_{U_B} < 235 K) is dominant during the initial hours of climactic eruptions on 15 Jan 2022. (b) The frequency histogram of $BT_{11.2\mu m}$ on 15 January 2022 at 08:40 UTC, when two umbrella clouds distinctly appear (as seen in Fig. 1d). (c) Same as (a) but at 11:50 Z when climactic eruptions started waning out.

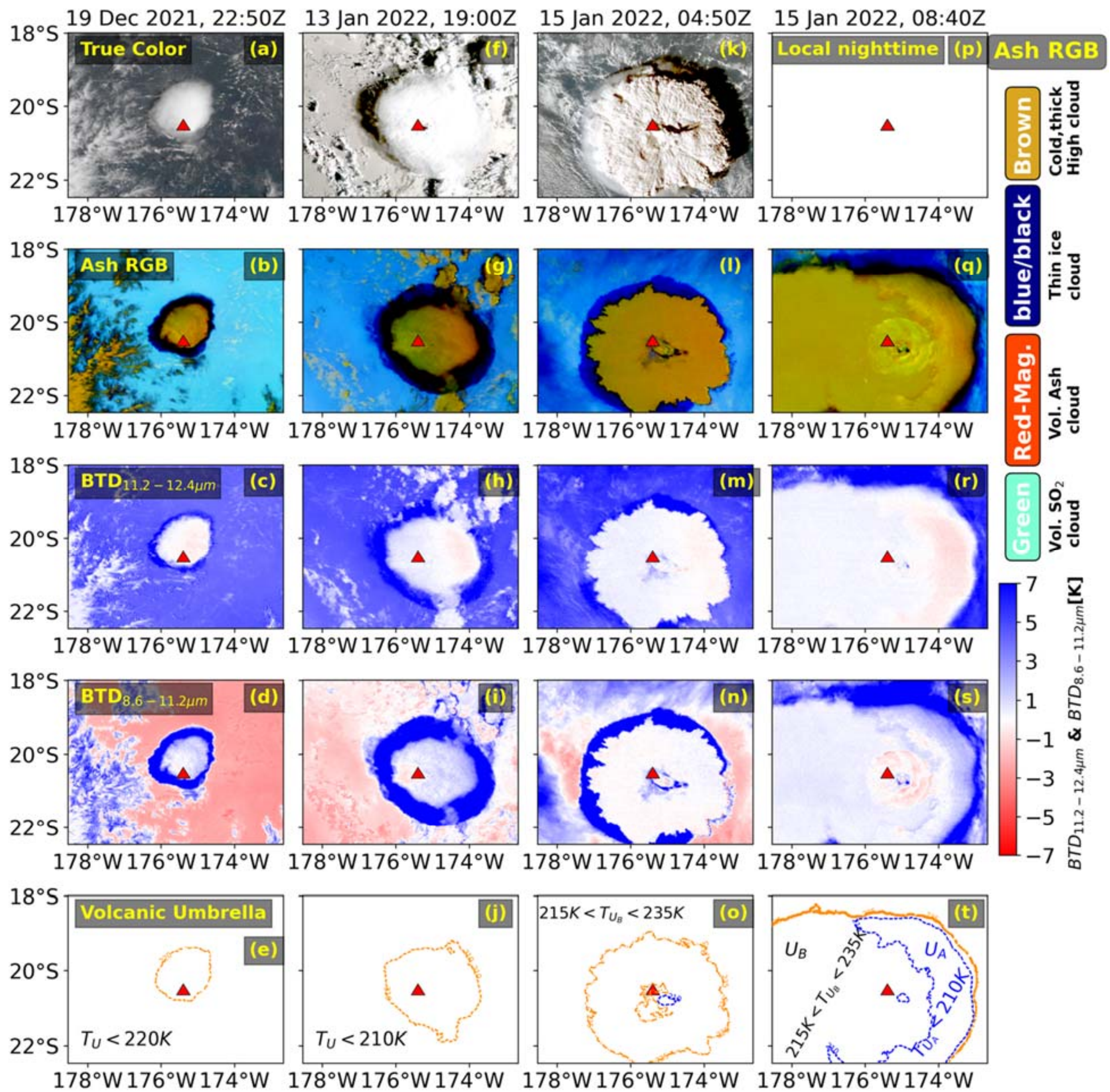

Figure 3: (a) Himawari-8 observed true color RGB centered around Hunga Tonga-Hunga Ha'apai (HTHH) (175.38°W, 20.57°S) submarine volcano on 19 December 2021 at 22:50 UTC. Panel (f), and (k) are similar to panel (a) but for 13 January 2022 at 19:00 UTC, 15 January 2022 at 04:50 UTC, respectively. Panel (p) is same as panel (k) but at 08:40 UTC. Also, there are no reflectance data during local nighttime at 08:40 UTC. Panel (b, g, l, q) same as (a, f, k, p) but for Ash RGB. (c) Himawari-8 observed brightness temperature difference between 11.2-12.4µm (BTD$_{11.2\text{-}12.4\mu m}$) on 19 December 2021 at 22:50 UTC. Panel (h), (m) and (r) are similar to panel

(c) but for 13 January 2022 at 19:00 UTC, 15 January 2022 at 04:50 UTC, 15 January 2022 at 08:40 UTC, respectively. Panel (d, i, n, s) same as (c, h, m, r) but for brightness temperature difference between 8.6-11.2μm ($BTD_{8.6\text{-}11.2\mu m}$). (e) the contour level extracted using a histogram technique (see Methods) on 19 December at 2250 UTC. (j) same as (e) but for 13 January 19:00Z at contour level 210 K. (o) same as (e) but for 15 January at 04:50 Z at 215K < T_{U_B} < 240K. (t) same as (o) but at 08:40 Z and for two contour levels (215K < T_{U_B}< 240K and T_{U_A}< 210K.

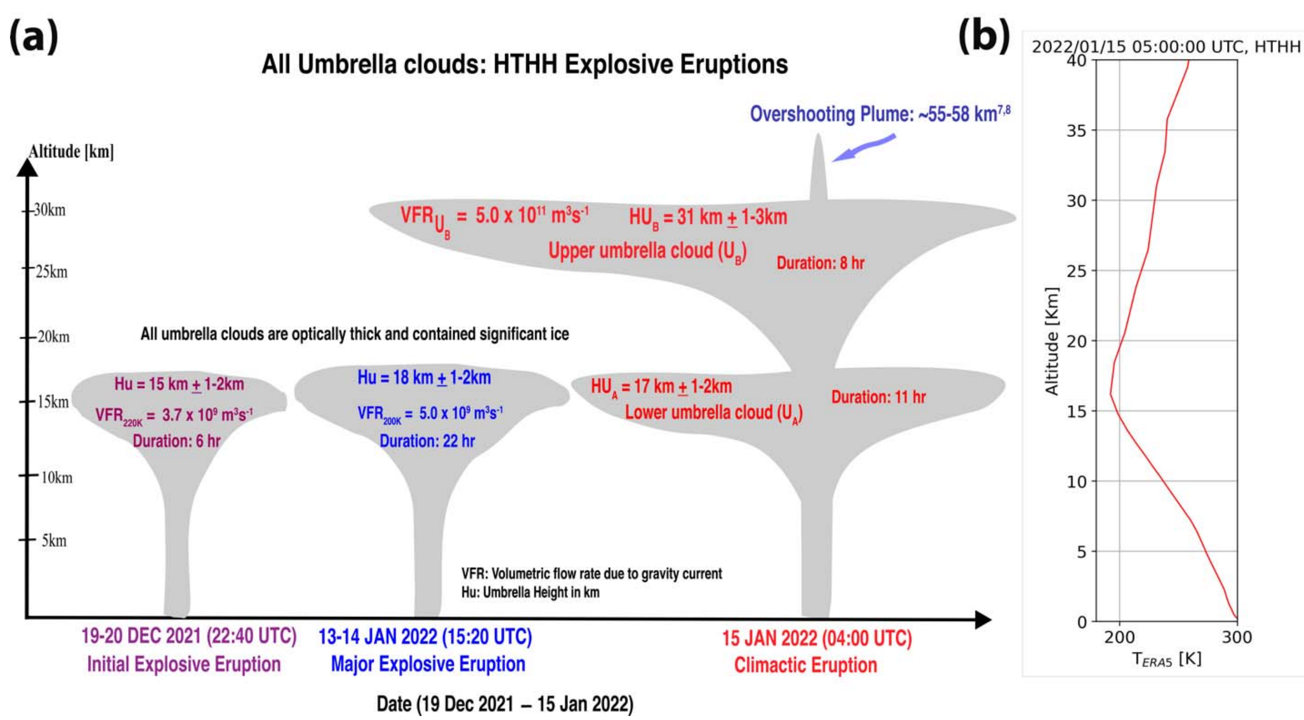

Figure 4: (a) Schematic summarizing our findings related to HTHH explosive eruptions. (b) Typical clear-sky temperature profile on 15 January 2022 at 05:00:00 UTC over HTHH.

Supplementary Materials for

Timelines of plume characteristics of the Hunga Tonga-Hunga Ha'apai eruption sequence from 19 December 2021 to 16 January 2022: Himawari-8 observations

Authors: Ashok Kumar Gupta[1*], Ralf Bennartz[1,2], Kristen E. Fauria[1], Tushar Mittal[3,4]

Affiliations:

[1]Department of Earth and Environmental Sciences, Vanderbilt University; Nashville, Tennessee, USA

[2]Space Science and Engineering Center, University of Wisconsin - Madison, Wisconsin, USA

[3]Department of Earth, Atmospheric and Planetary Sciences, Massachusetts Institute of Technology, Cambridge, Massachusetts, USA

[4]Department of Geosciences, Pennsylvania State University, Pennsylvania, USA

***Corresponding author. Email: ashok.k.gupta@vanderbilt.edu**

This PDF file includes:

Materials and Methods

Captions for Movies S1 to S8

Figs. S1 to S5

Supplementary Text

Materials and Methods

Minimum Brightness Temperature—BT_{min}:

For determining the umbrella cloud-top temperature, the $BT_{11.2\mu m}$ is an important parameter due to its strong transmissivity, which helps minimize the influence of the atmosphere above the umbrella clouds. In other words, the brightness temperature at 11.2μm ($BT_{11.2\mu m}$) is approximately proportional to the umbrella cloud-top or surface temperature because of the minimal atmospheric absorption. This minimal absorption at 11.2μm is primarily due to the water vapor[16,17]. For the explosive eruptions, the parallax correction in the $BT_{11.2\mu m}$ is not considered as the coverage of umbrella clouds was more dominant than the overshooting tops, which generally exhibits a stronger parallax effect.

To identify the start of an eruption and overshooting top location, we use the minimum brightness temperature values. Minimum brightness temperature can be used because plume overshoot can produce plumes that are colder than any point in the atmosphere and can also be useful to detect eruptive activity. For our case, the BT_{min} was taken within 2000 x 1245 pixels (e.g., the entire area covered in Figure 1d) enclosing the vent site.

True color and Ash RGBs and BTD tests

We first employed true color and ash RGBs (see Methods) to determine the umbrella's compositional characteristics. To create natural color RGBs suitable for human eyes to distinguish the volcanic features from Himawari-8 observation, we use reflectance at 0.47 (blue channel), 0.51 (green channel), and 0.64 (red channel). We set the color enhancement gamma value as 3 to bring out the bright and distinguishable true color RGB (Figure 3a-c). These RGBs composites were initially developed by European Organization for the Exploitation of Meteorological Satellites **(**EUMETSAT)[49,50]. We used infrared window channels such as 8.6μm, 10.4μm, and 12.4μm from Himawari-8 to create ash RGBs[49,50].

A channel at 8.6μm is particularly useful because of the higher volcanic ash absorption at 8.6μm relative to 11.2μm and 12.4μm[26,27]. The channels at 11.2μm and 12.4μm have opposite characteristics of absorption and scattering of water and quartz (present in volcanic ash) contents in the umbrella[26,27]. Therefore, for discriminating volcanic ash with ice clouds, we first use the reverse absorption technique[21,23,24] related to channels at 11.2μm and 12.4μm with some limitations (see Methods). However, using the reverse absorption technique to identify the umbrella clouds' composition, such as volcanic ash, can be misleading when volcanic ash is present in optically thick umbrella clouds (with strong temperature inversion), and occurs in a humid environment (such as in the tropics), mixed with ice/water clouds, and exhibits a relatively larger size[21,26,27]. We try to address some of these challenges by also using tri-spectral channels brightness temperature difference tests (e.g., $BTD_{11.2\text{-}12.4\mu m}$ vs. $BTD_{8.6\text{-}11.2\mu m}$) for interpreting the phase and optical properties of umbrella's composition other than RGBs. For instance, a strong positive value of $BTD_{8.6\text{-}11.2\mu m}$ relative to the $BTD_{11.2\text{-}12.24\mu m}$ could indicate the presence of ice clouds. A strong negative value of $BTD_{11.2\text{-}12.24\mu m}$ could indicate the presence of ash clouds within certain limitations described above.

Domain average method—Umbrella Cloud heights:

We take domain average (174.78°W–175.84°W; 21.00°S–20.25°S; magenta box in Figure S1) brightness temperature at 11.2μm (BT_{avg}) and convert the BT_{avg} into the height based ERA5 data[9]. This method allows us to determine the altitude of the cloud tops associated with volcano eruption provided that the averaging domain is devoid of meteorological clouds contamination as it can influence the BT_{avg} values.

Supplementary Movies S1 to S8

Movie S1:
The 10-min time-series of brightness temperature at 11.2μm ($BT_{11.2\mu m}$) over the HTHH site covering 19-20 December 2021 (initial eruption), 13-14 January 2022 (major eruption), and 15 January 2022 (Climactic eruption).

Movie S2:

Daytime true color RGB over the HTHH site covering 19-20 December 2021 (initial eruption),13-14 January 2022 (major eruption), and 15 January 2022 (Climactic eruption).

Movie S3:

The 10-min time-series of Ash RGB over the HTHH site covering 19-20 December 2021 (initial eruption), 13-14 January 2022 (major), and 15 January 2022 (Climactic).

Movie S4:

The brightness temperature difference between 11.2μm and 12.4μm over the HTHH site at the time-interval of 10-min during 19-20 December 2021 (initial eruption),13-14 January 2022 (major), and 15 January 2022 (Climactic).

Movie S5:

Same as Movie S6 but for brightness temperature difference between 8.6μm and 11.2μm.

Movie S6:

Same as Movie S3 but for different dates between 21 December 2021 and 12 January 2022.

Movie S7:

Left panel: the frequency histogram of $BT_{11.2\mu m}$ estimated for the entire area of Figure 1d for all values of $BT_{11.2\mu m}$ on 15 January 2022. Right panel: same as above but for $BT_{11.2\mu m}$ >270K.

Movie S8:

The extracted umbrella clouds based on histogram and image segmentation techniques (see Method section) for 15 January 2022 during 04:00-12:50 UTC. The part of lower umbrella cloud (U_A) is visible at 05:30 UTC as upper umbrella (U_B) moves westward. The red triangle marks the HTHH vent.

Supplementary Figures

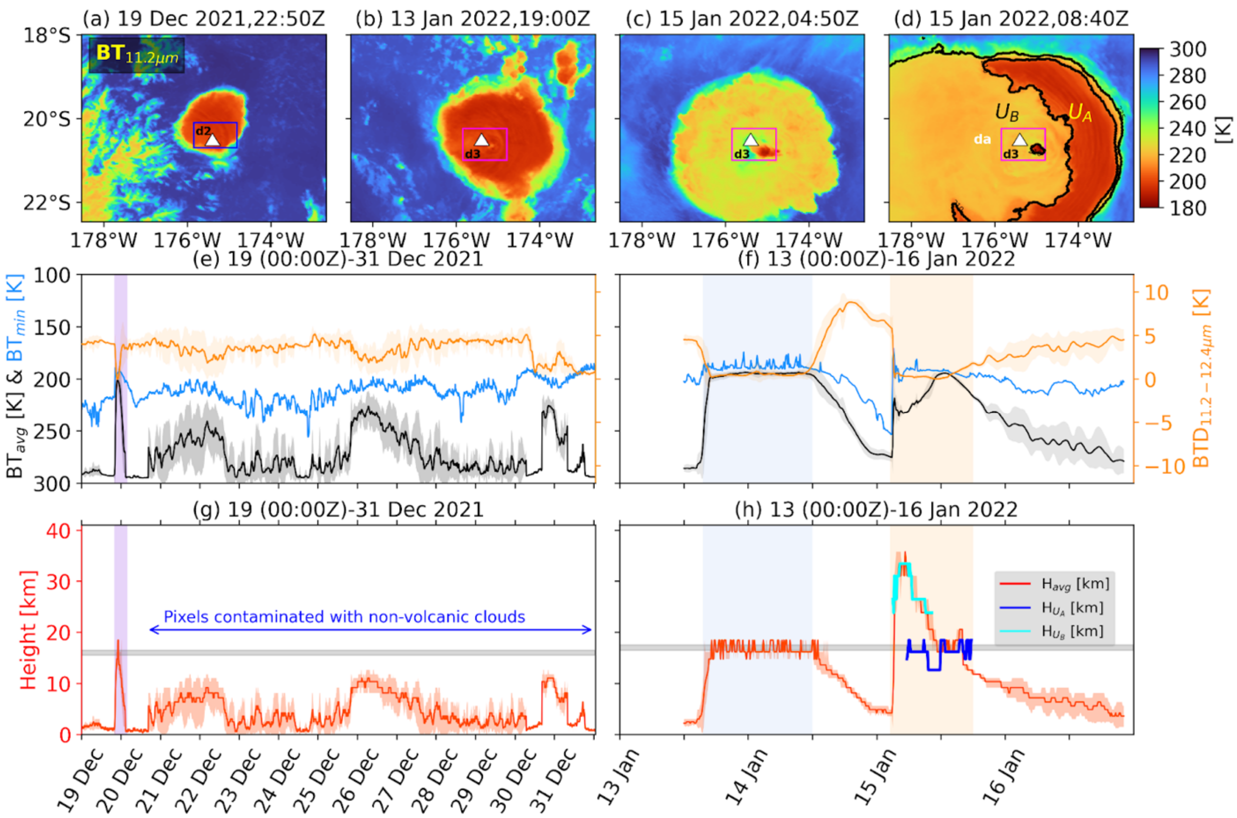

Figure S1: Based on box averaging method, the plumes moved towards the northeast and the averaged plume top heights within grid-box varied between 8 and 12 km (Figure S1a-d). **Upper panels**: same as the corresponding upper panels of Figure S1. The white triangle is centered around Hunga Tonga-Hunga Ha'apai (HTHH) (175.38°W, 20.57°S) submarine volcano. The blue box (175.84°W–174.80°W; 20.70°S–20.1°S) on 19 Dec 2021 and magenta box (174.78°W–175.84°W; 21.00°S–20.25°S) on 13-15 Jan 2022 are selected for estimating BT_{avg} on 19-31 December 2021, 13-15 January 2022 (see middle and bottom panels). The contour U_A is outlined for $BT_{11.2\mu m} < 210K$, and contour U_B is outlined for $215K < BT_{11.2\mu m} < 235K$. **Middle panels**: (e) the black line (BT_{avg}) indicates the timelines of the domain averaged (blue box on 19-31 December & magenta box on 13-16 January 2022) $BT_{11.2\mu m}$. The sky-blue line represents the minimum $BT_{11.2\mu m}$ (BT_{min}) covering entire pixels in Figure S1(a) centered over HTHH volcano during 19-31 December 2021. Similarly, the orange color indicates the BT difference between 11.2 and 12.4µm ($BTD_{11.2\text{-}12.4\mu m}$). (f) The black, orange, and sky-blue lines represent the same quantities as in panel e. **Bottom panels**: (g-h) The red line indicates the satellite-derived volcanic clouds height in km (sometimes contaminated with non-volcanic clouds) based on the BT_{avg} value and ERA5 data above. The blue and cyan lines indicate contour U_A and contour U_B umbrella heights (depicted in panel d) for the eruption on 15 January 2022.

We applied the average domain technique to find the average brightness temperature (BT_{avg}) associated with pulses of plumes (21-31 Dec 2021) and umbrella clouds (19-20 Dec 2021, 13-14 Jan 2022, 15 Jan 2022). The selected domain surrounding the regions of HTHH's vent is highlighted by a rectangular box enclosing the HTHH's vent. The magenta rectangular box covers area (174.78°W–175.84°W; 21.00°S–20.25°S) that encloses the parallax effect. However, estimating plume/umbrella top temperature using the average domain technique can produce significant biasing, especially when the eruption activity is weak, and we have an irregular pulse of plumes. Figure S1e, f shows the large deviation in the BT_{avg} during Dec 21-31, 2021. During this period, the HTHH eruptions were not so explosive that they could not produce umbrella clouds. Due to a large deviation in BT_{avg}, the satellite-derived umbrella height also exhibits a large uncertainty, as evident from Fig. S1g, h.

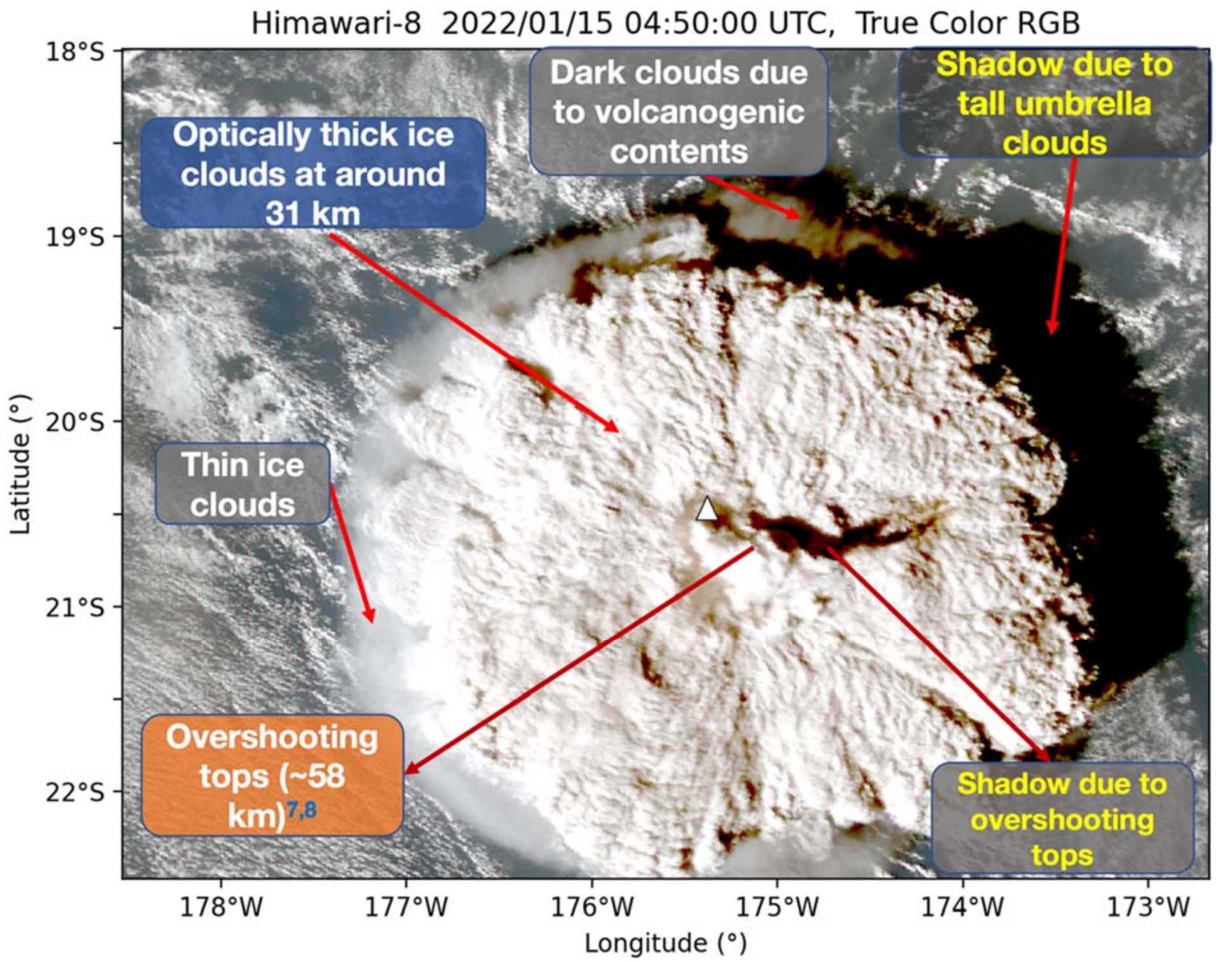

Figure S2: Visual imagery of the HTHH explosive eruption on 15 January 2022 at 04:50 UTC. Different features of volcanic clouds are highlighted.

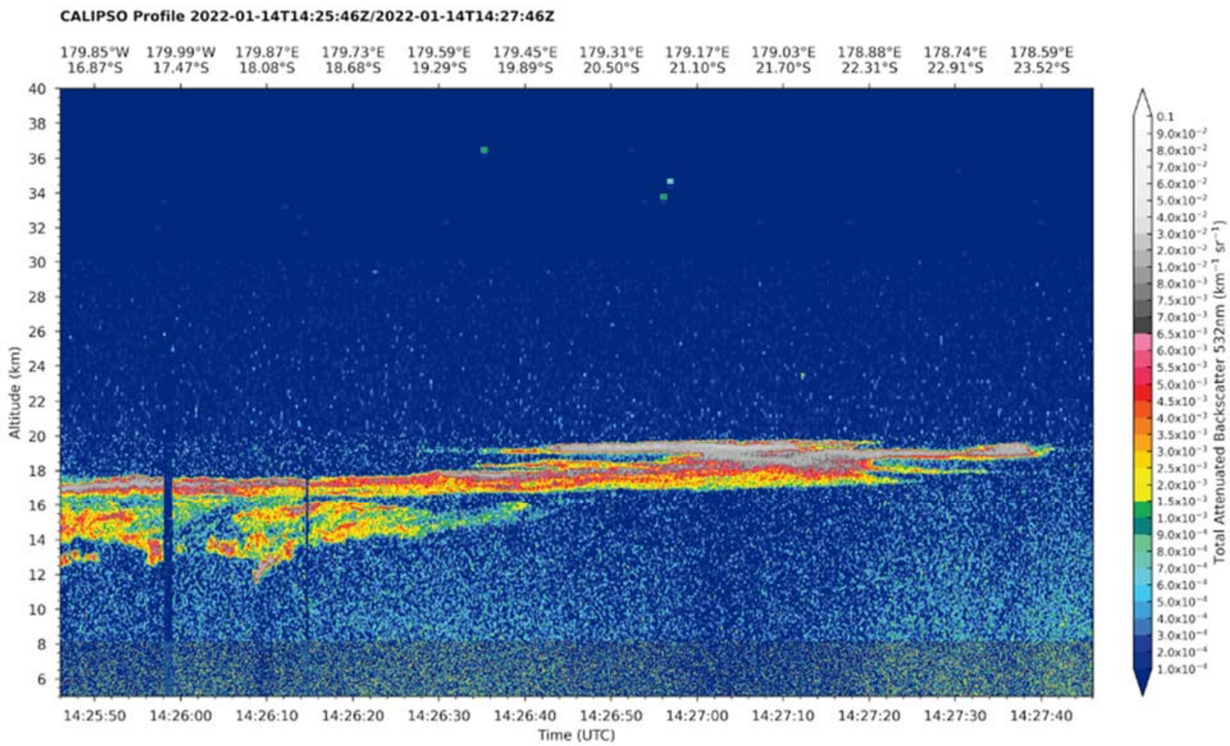

***Figure S3**:*

During major eruption between 13-14 January 2022, the total attenuated backscatter at 532 nm from CALIPSO shows that the HTHH related plume reached up to ~19km.

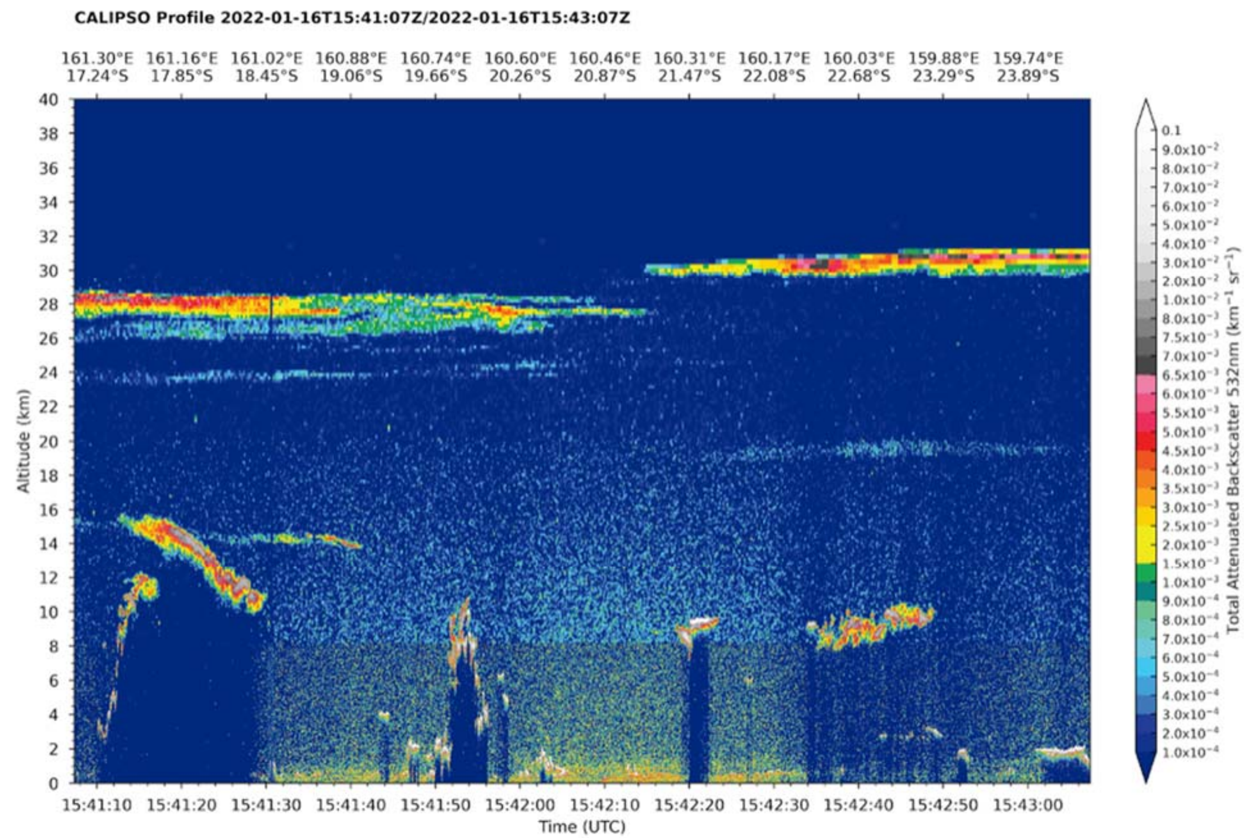

Figure S4:

Same as Figure S3 but after the climactic eruption on 16 January 2022 at 15:41 UTC.

It shows that the plume altitude reached up to ~31 km.

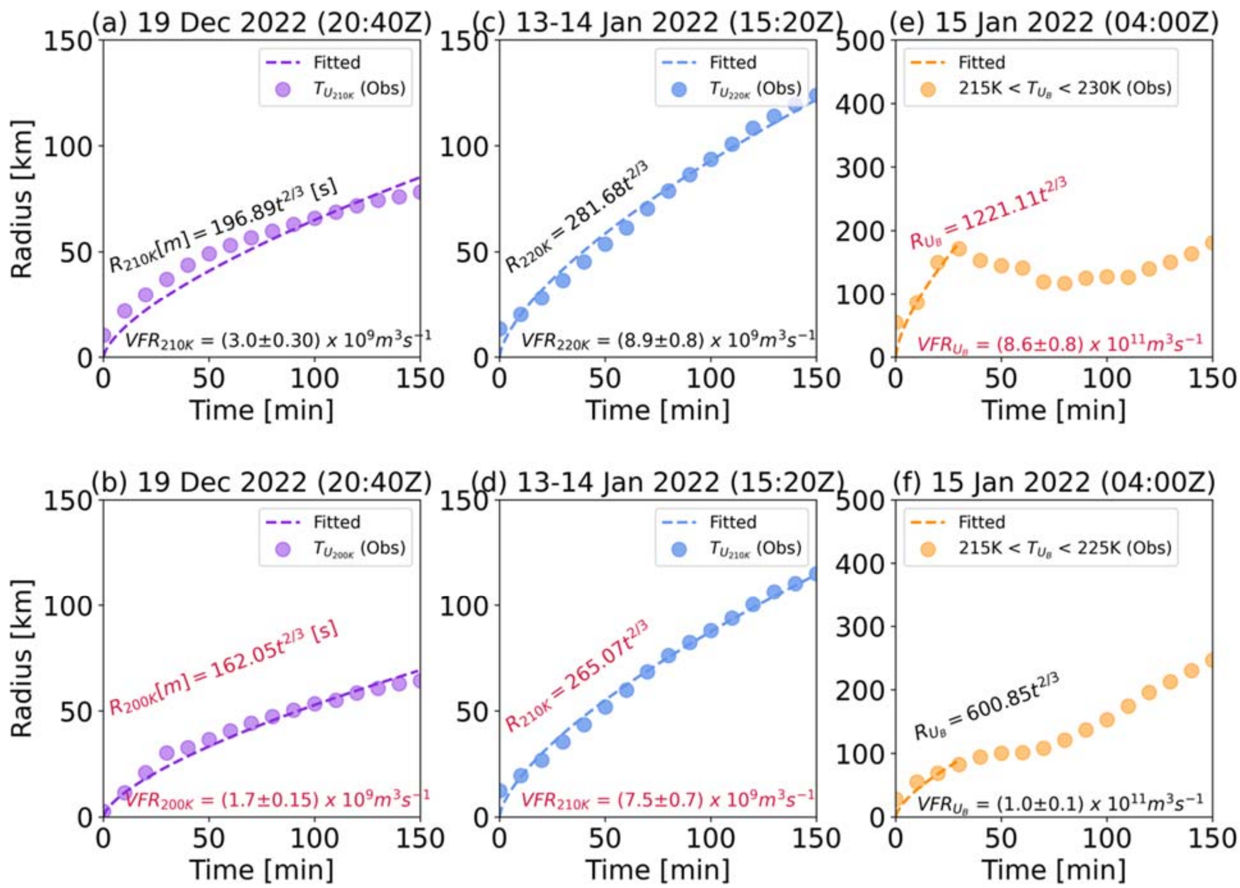

Figure S5: Volumetric flow rate (VFR) is estimated for the contour labeled at: (a) 210K (b) 220K on 19 December 2021 for the initial 150 mins from Himawari-8 observations (Obs); (c) 220 K and (d) 210 K on 13 January 2022 for the initial 150 mins; (e) 215K < T_{U_B}< 240K and (f) 215K < T_{U_B}< 240K on 15 January 2022 for the initial 50 mins. The mean and uncertainty numbers are rounded.

Using other contour levels, umbrella cloud areas over the first 150 minutes of the eruption on 19 Dec 2021 for contour levels at 210 K (Fig. S5a) and 200 K (Fig. S5b) are slightly reduced. The VFR was found to be 3.0 ± 0.60 x 10^9 m^3s^{-1} at 210 K (Fig. S5a) and (1.7 ± 0.15) x 10^9 m^3s^{-1} at 200 K (Fig. S5b), respectively. These slight reductions in VFR values are indicative in the uncertainty in VFR associated with different choices in contour levels and hence the areal coverage.

At different contour levels of 210K and 220K, the VFR on 13 Jan 2022 is increased by more than 50% relative to the contour level of 200K due to larger area coverage by umbrella clouds within the first 150 min (Figure S5c, d).

For contour levels between 215 and 230 K, the VFR for U_B is 72% (Figure S5e) higher than the estimated value between 215 and 235 K contour levels (Figure 2c).

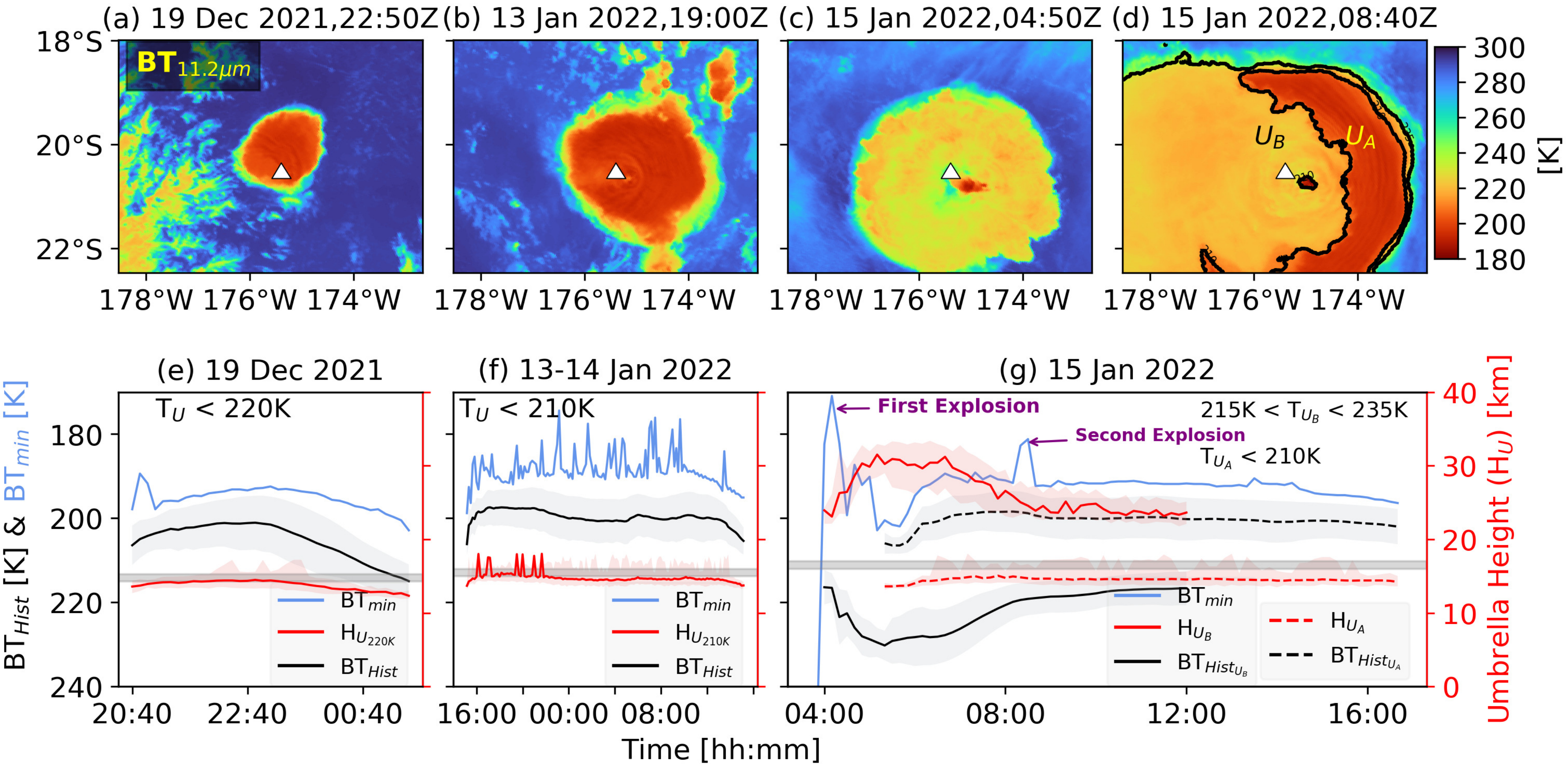

(a) 19 Dec 2021,22:50Z
(b) 13 Jan 2022,19:00Z
(c) 15 Jan 2022,04:50Z
(d) 15 Jan 2022,08:40Z
BT11.2μm
18°S
20°S
22°S
178°W 176°W 174°W
U_B
U_A
300
280
260
240
220
200
180
[K]
(e) 19 Dec 2021
(f) 13-14 Jan 2022
(g) 15 Jan 2022
T_U < 220K
T_U < 210K
215K < T_UB < 235K
T_UA < 210K
First Explosion
Second Explosion
BT_Hist [K] & BT_min [K]
Umbrella Height (H_U) [km]
BT_min
H_U220K
H_U210K
BT_Hist
H_UB
H_UA
BT_HistUB
BT_HistUA
20:40 22:40 00:40
16:00 00:00 08:00
04:00 08:00 12:00 16:00
Time [hh:mm]

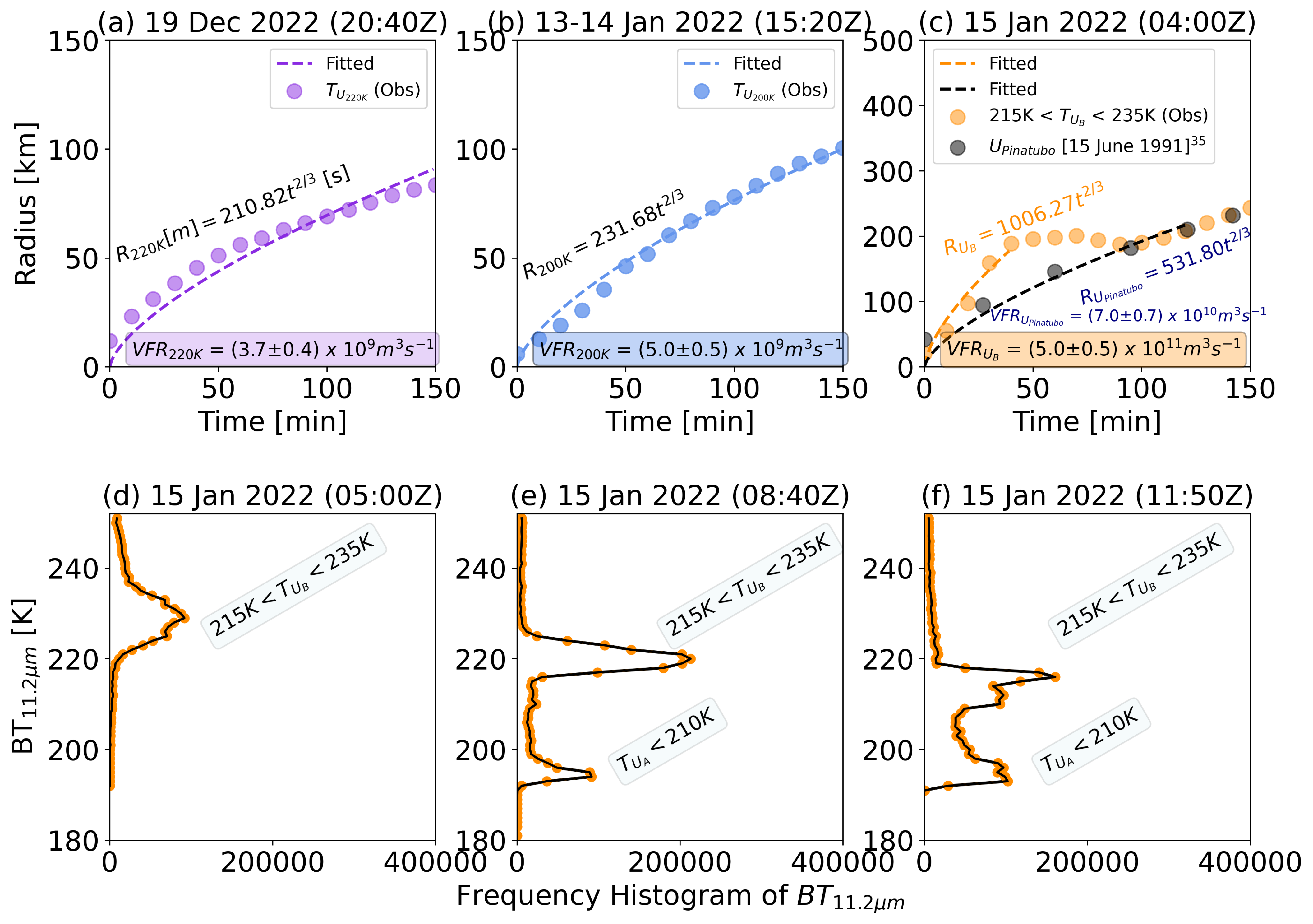

(a) 19 Dec 2022 (20:40Z)
(b) 13-14 Jan 2022 (15:20Z)
(c) 15 Jan 2022 (04:00Z)
Radius [km]
Time [min]
Fitted
$T_{U_{220K}}$ (Obs)
$T_{U_{200K}}$ (Obs)
$R_{220K}[m] = 210.82t^{2/3}$ [s]
$R_{200K} = 231.68t^{2/3}$
VFR_{220K} = (3.7±0.4) x $10^9 m^3 s^{-1}$
VFR_{200K} = (5.0±0.5) x $10^9 m^3 s^{-1}$
215K < T_{U_B} < 235K (Obs)
$U_{Pinatubo}$ [15 June 1991][35]
$R_{U_B} = 1006.27t^{2/3}$
$R_{U_{Pinatubo}} = 531.80t^{2/3}$
$VFR_{U_{Pinatubo}}$ = (7.0±0.7) x $10^{10} m^3 s^{-1}$
VFR_{U_B} = (5.0±0.5) x $10^{11} m^3 s^{-1}$
(d) 15 Jan 2022 (05:00Z)
(e) 15 Jan 2022 (08:40Z)
(f) 15 Jan 2022 (11:50Z)
$BT_{11.2\mu m}$ [K]
$215K < T_{U_B} < 235K$
$T_{U_A} < 210K$
Frequency Histogram of $BT_{11.2\mu m}$

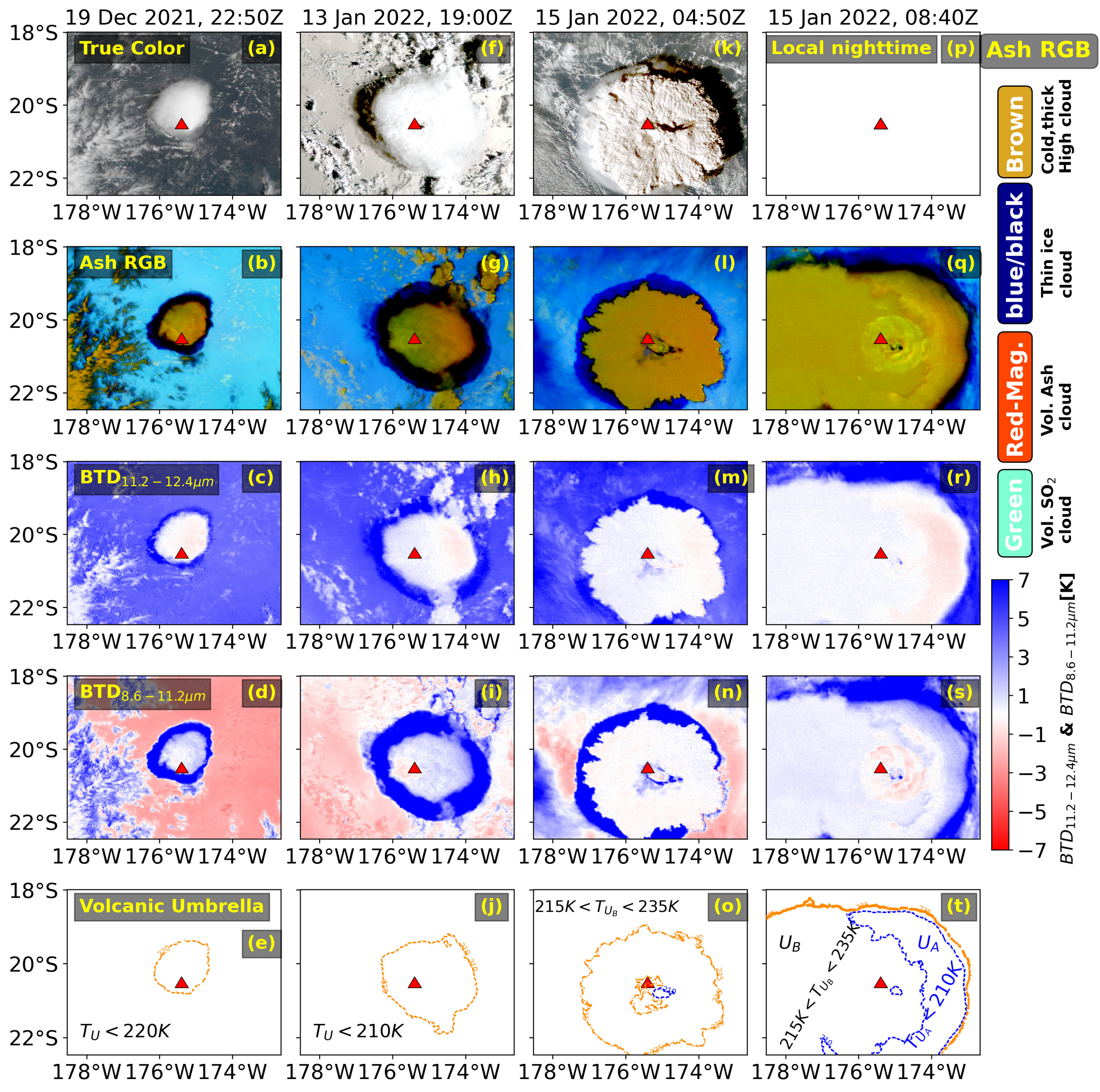

19 Dec 2021, 22:50Z
13 Jan 2022, 19:00Z
15 Jan 2022, 04:50Z
15 Jan 2022, 08:40Z
True Color
Local nighttime
Ash RGB
BTD$_{11.2-12.4\mu m}$
BTD$_{8.6-11.2\mu m}$
Volcanic Umbrella
(a) (b) (c) (d) (e) (f) (g) (h) (i) (j) (k) (l) (m) (n) (o) (p) (q) (r) (s) (t)
$T_U < 220K$
$T_U < 210K$
$215K < T_{U_B} < 235K$
U_B
U_A
$T_{U_A} < 210K$
Brown
Cold,thick High cloud
blue/black
Thin ice cloud
Red-Mag.
Vol. Ash cloud
Green
Vol. SO$_2$ cloud
$BTD_{11.2-12.4\mu m}$ & $BTD_{8.6-11.2\mu m}$[K]
7
5
3
1
−1
−3
−5
−7
18°S
20°S
22°S
178°W
176°W
174°W

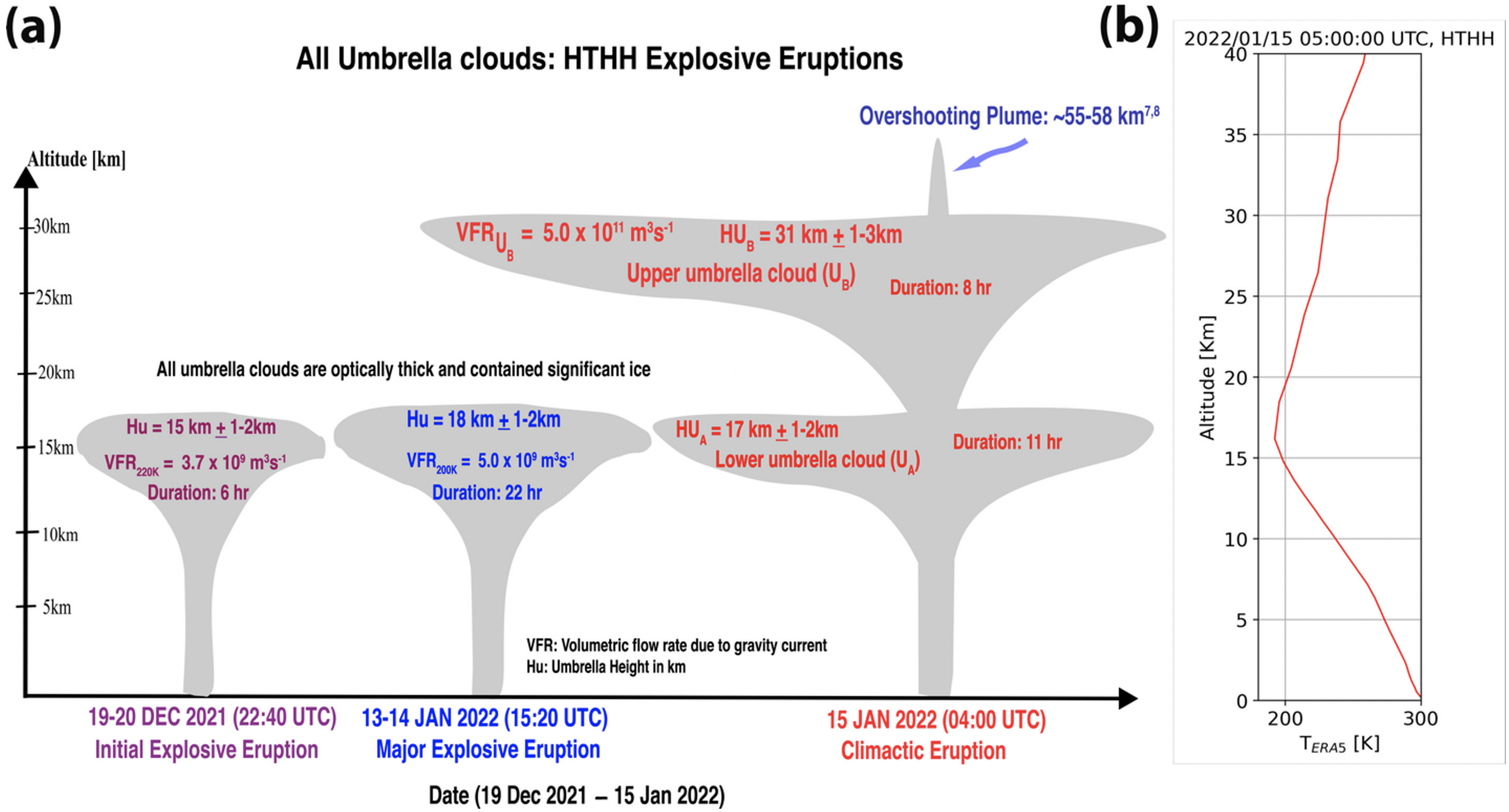

(a)
All Umbrella clouds: HTHH Explosive Eruptions
Overshooting Plume: ~55-58 km7,8
Altitude [km]
30km
25km
20km
15km
10km
5km
VFRUB = 5.0 x 10^11 m^3s^-1
HUB = 31 km ± 1-3km
Upper umbrella cloud (UB)
Duration: 8 hr
All umbrella clouds are optically thick and contained significant ice
Hu = 15 km ± 1-2km
VFR220K = 3.7 x 10^9 m^3s^-1
Duration: 6 hr
Hu = 18 km ± 1-2km
VFR200K = 5.0 x 10^9 m^3s^-1
Duration: 22 hr
HUA = 17 km ± 1-2km
Lower umbrella cloud (UA)
Duration: 11 hr
VFR: Volumetric flow rate due to gravity current
Hu: Umbrella Height in km
19-20 DEC 2021 (22:40 UTC)
Initial Explosive Eruption
13-14 JAN 2022 (15:20 UTC)
Major Explosive Eruption
15 JAN 2022 (04:00 UTC)
Climactic Eruption
Date (19 Dec 2021 – 15 Jan 2022)
(b)
2022/01/15 05:00:00 UTC, HTHH
Altitude [Km]
TERA5 [K]

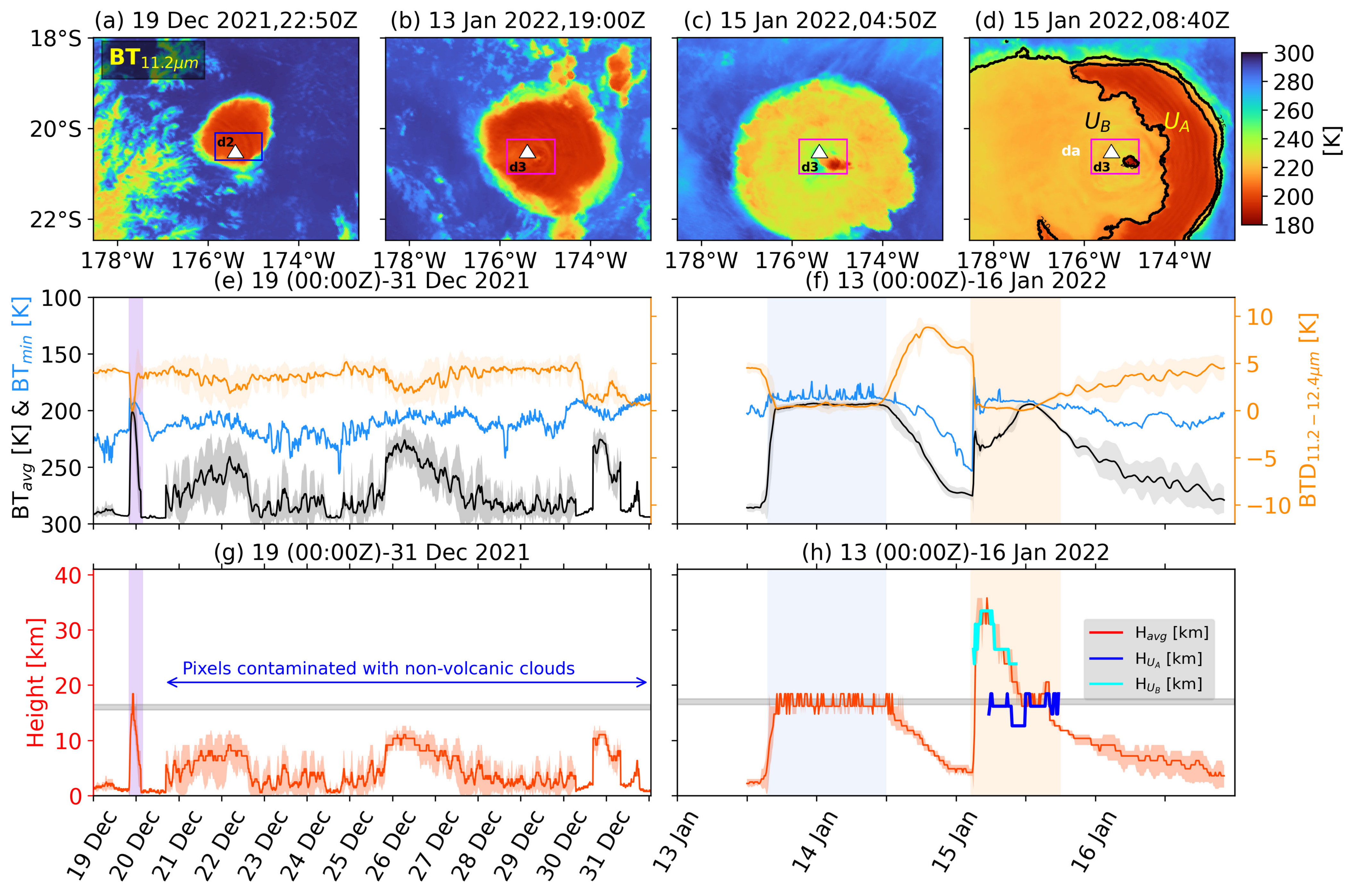

(a) 19 Dec 2021,22:50Z
(b) 13 Jan 2022,19:00Z
(c) 15 Jan 2022,04:50Z
(d) 15 Jan 2022,08:40Z
BT11.2μm
d2
d3
da
U_B
U_A
[K]
(e) 19 (00:00Z)-31 Dec 2021
(f) 13 (00:00Z)-16 Jan 2022
BTavg [K] & BTmin [K]
BTD11.2−12.4μm [K]
(g) 19 (00:00Z)-31 Dec 2021
(h) 13 (00:00Z)-16 Jan 2022
Height [km]
Pixels contaminated with non-volcanic clouds
Havg [km]
HUA [km]
HUB [km]

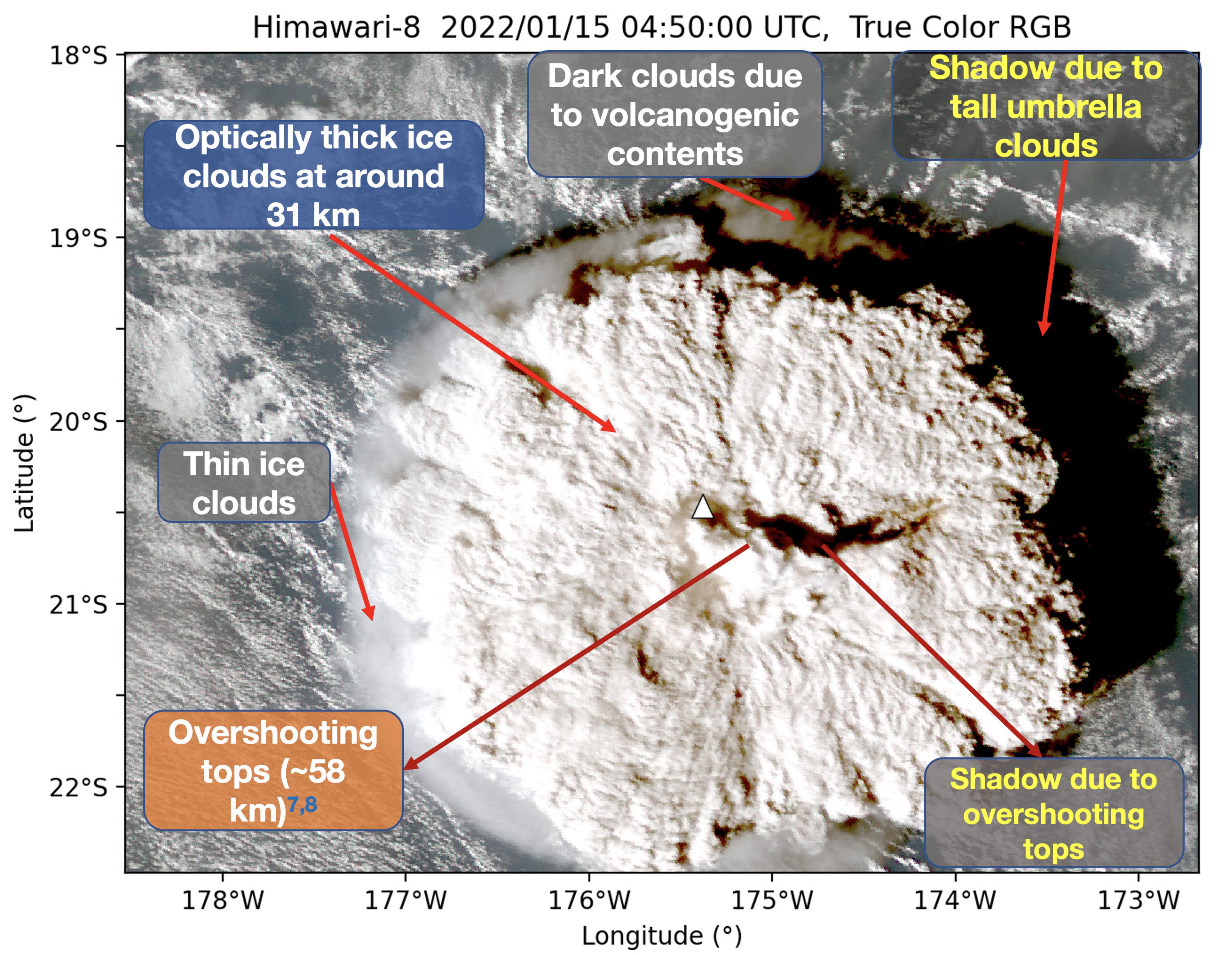
Himawari-8 2022/01/15 04:50:00 UTC, True Color RGB
Optically thick ice clouds at around 31 km
Dark clouds due to volcanogenic contents
Shadow due to tall umbrella clouds
Thin ice clouds
Overshooting tops (~58 km)[7,8]
Shadow due to overshooting tops
18°S
19°S
20°S
21°S
22°S
Latitude (°)
178°W
177°W
176°W
175°W
174°W
173°W
Longitude (°)

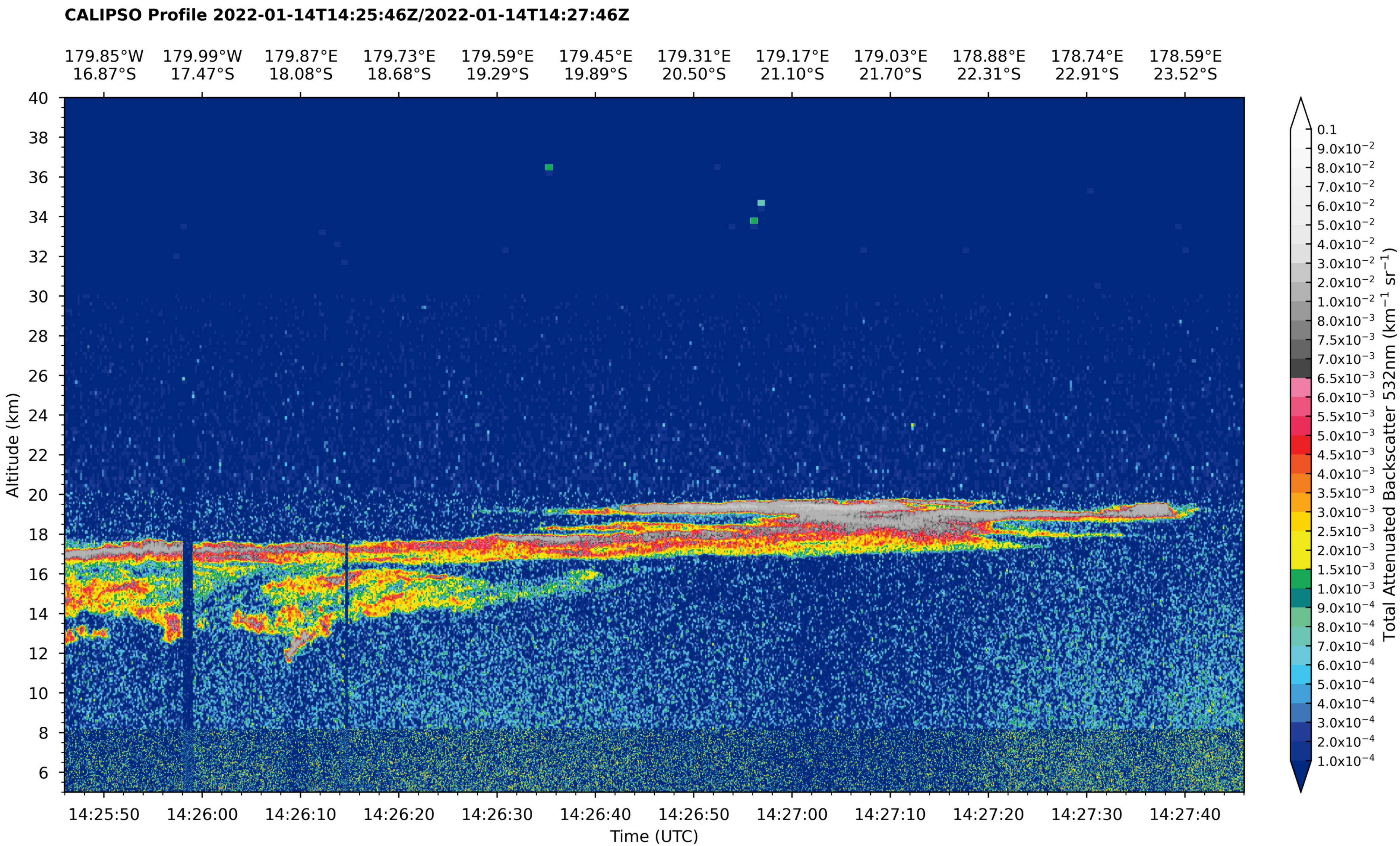

CALIPSO Profile 2022-01-14T14:25:46Z/2022-01-14T14:27:46Z
179.85°W 16.87°S
179.99°W 17.47°S
179.87°E 18.08°S
179.73°E 18.68°S
179.59°E 19.29°S
179.45°E 19.89°S
179.31°E 20.50°S
179.17°E 21.10°S
179.03°E 21.70°S
178.88°E 22.31°S
178.74°E 22.91°S
178.59°E 23.52°S
Altitude (km)
40
38
36
34
32
30
28
26
24
22
20
18
16
14
12
10
8
6
14:25:50
14:26:00
14:26:10
14:26:20
14:26:30
14:26:40
14:26:50
14:27:00
14:27:10
14:27:20
14:27:30
14:27:40
Time (UTC)
Total Attenuated Backscatter 532nm (km^{-1} sr^{-1})
0.1
9.0x10^{-2}
8.0x10^{-2}
7.0x10^{-2}
6.0x10^{-2}
5.0x10^{-2}
4.0x10^{-2}
3.0x10^{-2}
2.0x10^{-2}
1.0x10^{-2}
8.0x10^{-3}
7.5x10^{-3}
7.0x10^{-3}
6.5x10^{-3}
6.0x10^{-3}
5.5x10^{-3}
5.0x10^{-3}
4.5x10^{-3}
4.0x10^{-3}
3.5x10^{-3}
3.0x10^{-3}
2.5x10^{-3}
2.0x10^{-3}
1.5x10^{-3}
1.0x10^{-3}
9.0x10^{-4}
8.0x10^{-4}
7.0x10^{-4}
6.0x10^{-4}
5.0x10^{-4}
4.0x10^{-4}
3.0x10^{-4}
2.0x10^{-4}
1.0x10^{-4}

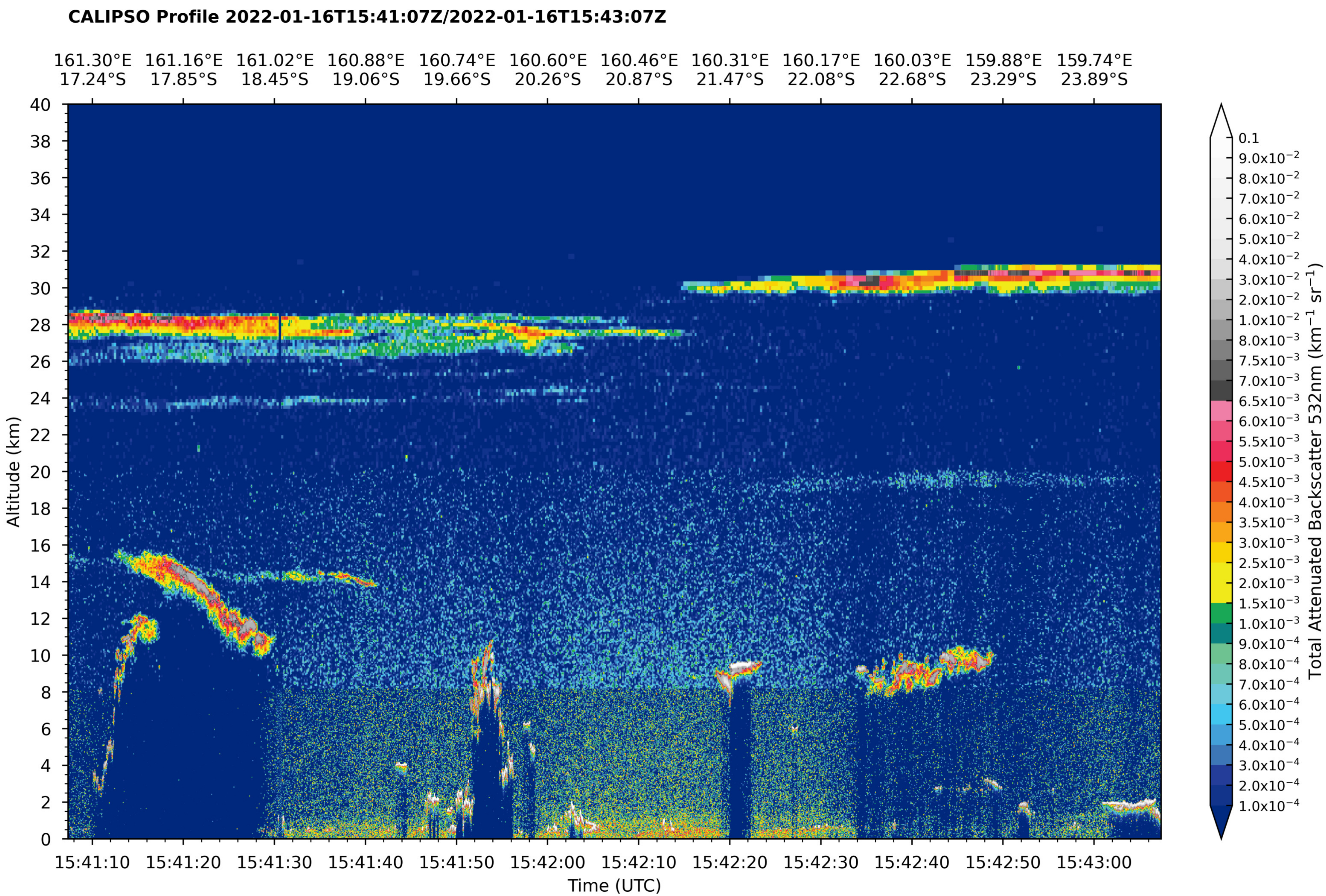
CALIPSO Profile 2022-01-16T15:41:07Z/2022-01-16T15:43:07Z
161.30°E 17.24°S
161.16°E 17.85°S
161.02°E 18.45°S
160.88°E 19.06°S
160.74°E 19.66°S
160.60°E 20.26°S
160.46°E 20.87°S
160.31°E 21.47°S
160.17°E 22.08°S
160.03°E 22.68°S
159.88°E 23.29°S
159.74°E 23.89°S
Altitude (km)
Time (UTC)
15:41:10
15:41:20
15:41:30
15:41:40
15:41:50
15:42:00
15:42:10
15:42:20
15:42:30
15:42:40
15:42:50
15:43:00
Total Attenuated Backscatter 532nm (km^{-1} sr^{-1})

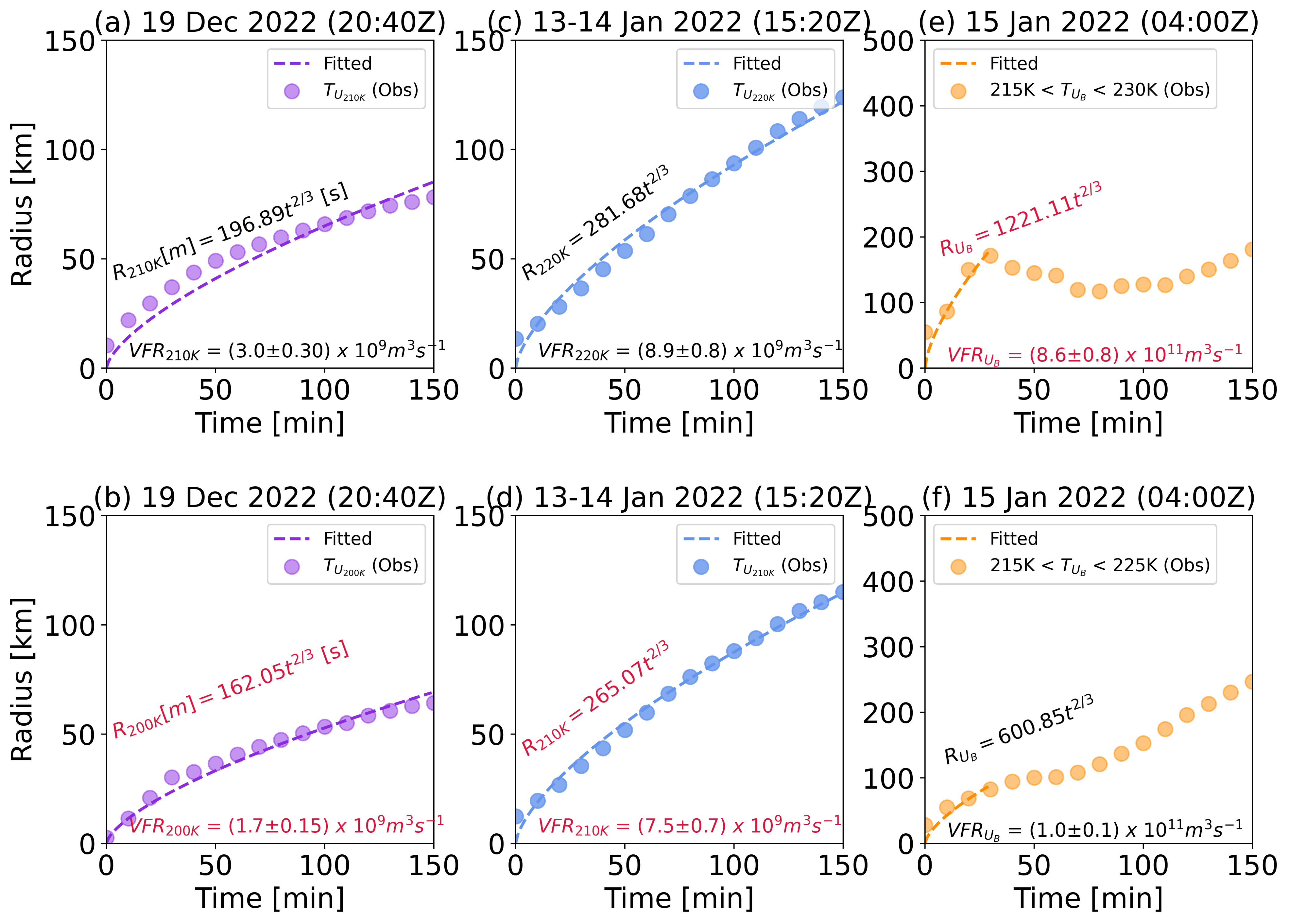

(a) 19 Dec 2022 (20:40Z)
Fitted
$T_{U_{210K}}$ (Obs)
$R_{210K}[m] = 196.89t^{2/3}$ [s]
VFR_{210K} = (3.0±0.30) x $10^9 m^3 s^{-1}$
(c) 13-14 Jan 2022 (15:20Z)
Fitted
$T_{U_{220K}}$ (Obs)
$R_{220K} = 281.68t^{2/3}$
VFR_{220K} = (8.9±0.8) x $10^9 m^3 s^{-1}$
(e) 15 Jan 2022 (04:00Z)
Fitted
215K < T_{U_B} < 230K (Obs)
$R_{U_B} = 1221.11t^{2/3}$
VFR_{U_B} = (8.6±0.8) x $10^{11} m^3 s^{-1}$
(b) 19 Dec 2022 (20:40Z)
Fitted
$T_{U_{200K}}$ (Obs)
$R_{200K}[m] = 162.05t^{2/3}$ [s]
VFR_{200K} = (1.7±0.15) x $10^9 m^3 s^{-1}$
(d) 13-14 Jan 2022 (15:20Z)
Fitted
$T_{U_{210K}}$ (Obs)
$R_{210K} = 265.07t^{2/3}$
VFR_{210K} = (7.5±0.7) x $10^9 m^3 s^{-1}$
(f) 15 Jan 2022 (04:00Z)
Fitted
215K < T_{U_B} < 225K (Obs)
$R_{U_B} = 600.85t^{2/3}$
VFR_{U_B} = (1.0±0.1) x $10^{11} m^3 s^{-1}$
Radius [km]
Time [min]